How to cite: *Angew. Chem. Int. Ed.* **2025**, *64*, e202418431
doi.org/10.1002/anie.202418431

Artificial Cells

Synthetic Biomolecular Condensates: Phase-Separation Control, Cytomimetic Modelling and Emerging Biomedical Potential

Siyu Song, Tsvetomir Ivanov, Thao. P. Doan-Nguyen, Lucas Caire da Silva, Jing Xie, Katharina Landfester,* and Shoupeng Cao**

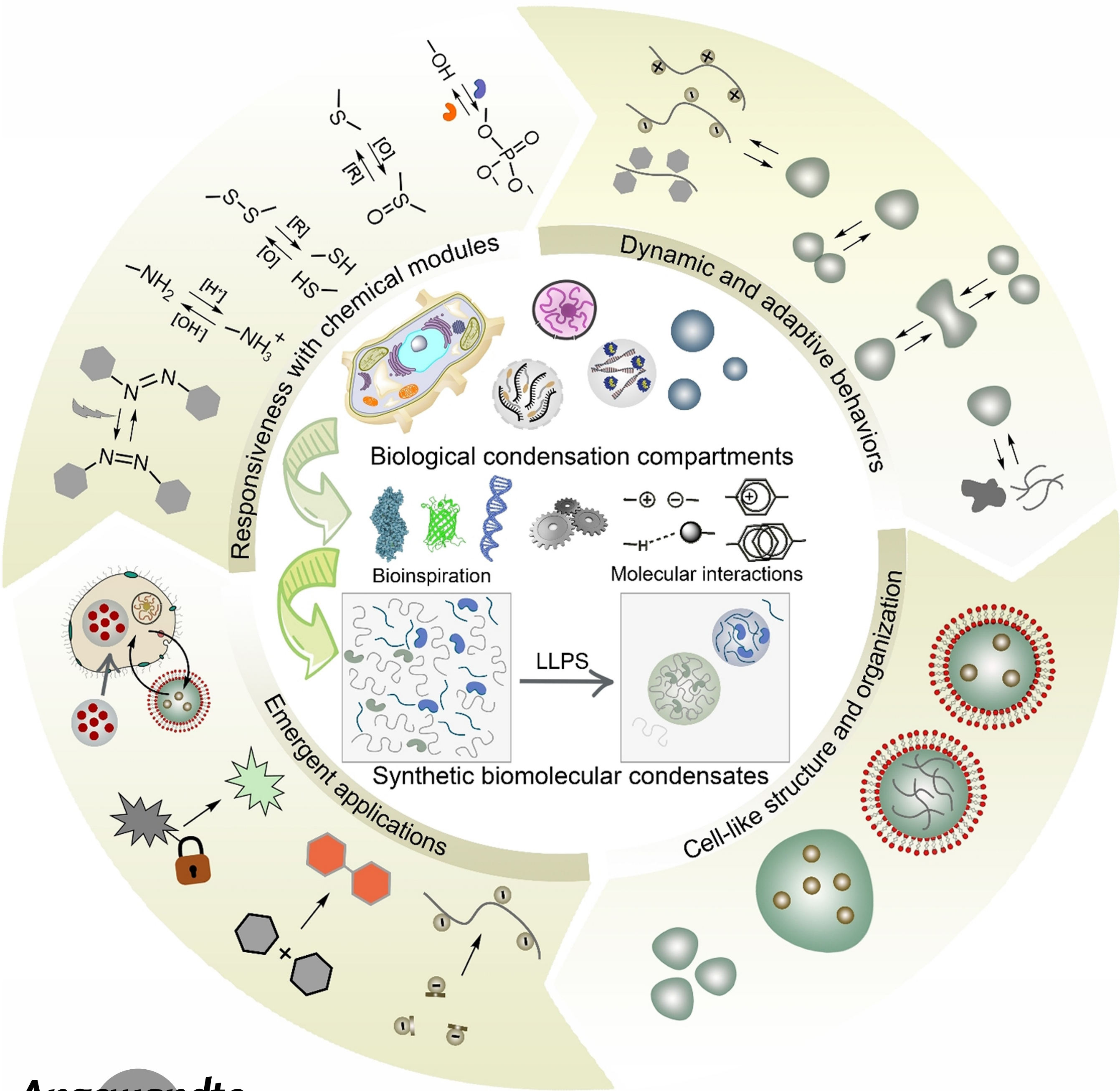

Abstract: Liquid-liquid phase separation towards the formation of synthetic coacervate droplets represents a rapidly advancing frontier in the fields of synthetic biology, material science, and biomedicine. These artificial constructures mimic the biophysical principles and dynamic features of natural biomolecular condensates that are pivotal for cellular regulation and organization. Via adapting biological concepts, synthetic condensates with dynamic phase-separation control provide crucial insights into the fundamental cell processes and regulation of complex biological pathways. They are increasingly designed with the ability to display more complex and ambitious cell-like features and behaviors, which offer innovative solutions for cytomimetic modeling and engineering active materials with sophisticated functions. In this minireview, we highlight recent advancements in the design and construction of synthetic coacervate droplets; including their biomimicry structure and organization to replicate life-like properties and behaviors, and the dynamic control towards engineering active coacervates. Moreover, we highlight the unique applications of synthetic coacervates as catalytic centers and promising delivery vehicles, so that these biomimicry assemblies can be translated into practical applications.

1. Introduction

Intracellular liquid-liquid phase separation (LLPS) is increasingly recognized to be closely associated with the formation of membrane-less organelles, also known as biomolecular condensates, such as germ granules, Cajal Bodies, and the nucleolus in living cells.[1] These condensates typically form from a mixture of proteins and nucleic acids spontaneously upon reaching a saturation threshold through energetically favored associative interactions.[2] The phase separation yields biomolecular condensates as dense and crowded micro-sized droplets enriched with biomacromolecules with a surrounding diluted environment.[3] The condensates are ubiquitously involved in biological compartmentalization for cellular organization, a hallmark of eukaryotic life.[4] Due to their ability to spatially concentrate active biomolecules, biomolecular condensates play a key role in organizing the physical separation of important biochemical reactions and manipulating various intracellular processes including information storage, signal transduction, and function execution accordingly.[5] The reversible formation and highly dynamic properties of biomolecular condensates enable biochemical reactions and intracellular processes to happen at the right time and place.[6] This is of crucial importance in regulating various cellular functions and behaviors, including but not limited to ribosome biogenesis, protein expression, stress response, and deoxyribonucleic acid (DNA) replication.[7] In addition, protein misfolding and amyloid nucleation through liquid-liquid phase separation are also closely associated with a series of health-related diseases, including cancer.[8] The significant biological roles of intracellular condensates inspired synthetic biology communities to create artificial analogs, known as synthetic biomolecular condensates that can utilize biological principles, mimic intracellular complexity, and replicate life-like properties and behaviors.[9]

Synthetic coacervate-based liquid microdroplets via a bottom-up approach have emerged to be powerful candidates in resembling the phase-separation behaviors and biophysical features of biomolecular condensates.[10] Adapting biological principles enables the facile design of synthetic coacervates as life-like compartments with distinct chemical compositions and structures.[11] This makes it feasible to precisely manipulate intra/inter-molecular interactions and fine-tune the macroscopic physical properties, such as size, viscosity, polarity, rheology, fluidity, and charge of the synthetic condensates.[12] Importantly, the most intriguing properties and features of synthetic condensates are the facile integration of responsive modules that render adaptive behaviors and life-like features.[13] The facile exploration and utilization of dynamic characters in synthetic coacervates offer many unique and important merits, making them highly appealing candidates for engineering adaptive biomimetic models.[14] Due to their similarity with biomolecular condensates, synthetic coacervates represent an alternative paradigm to unravel the fundamental molecular interactions and chemical mechanisms underlying the biological LLPS.[15] This enables a deeper understanding of the biological complexity and complicated intracellular behaviors for fundamental investigations from a molecular level.[16] Upon

[*] Prof. Dr. S. Cao
College of Polymer Science and Engineering, State Key Laboratory of Polymer Materials Engineering, Sichuan University, Chengdu 610065, PR China
E-mail: caoshoupeng@scu.edu.cn

Dr. S. Song
Life-Like Materials and Systems, Department of Chemistry, University of Mainz, 55128, Mainz, Germany

T. Ivanov, Dr. T. P. Doan-Nguyen, Prof. Dr. L. C. da Silva, Prof. Dr. K. Landfester
Max Planck Institute for Polymer Research, 55128 Mainz, Germany
E-mail: landfester@mpip-mainz.mpg.de

Prof. Dr. J. Xie
Institute of Biomedical Engineering, West China School of Basic Medical Sciences & Forensic Medicine, Sichuan University, Chengdu 610041, PR China
E-mail: jingxie@scu.edu.cn

Dr. T. P. Doan-Nguyen
International Center for Young Scientists, National Institute for Materials Science, 1-2-1 Sengen, Tsukuba, Ibaraki 305-0047, Japan

Prof. Dr. L. C. da Silva
Department of Chemistry, McGill University, Montreal H3A 0B8, Canada

integration with intracellular complexity and life-like properties, synthetic coacervate droplets can be rationally designed into advanced materials with sophisticated functions.[17] The ability to spatially partition and concentrate a wide range of functional species in synthetic condensates makes them an ideal platform as regulating

Siyu Song received her PhD from the Northwest A&F University under the supervision of Prof. Zhichao Pei. Her PhD thesis mainly covered the fabrication, functionalization, and application of quartz crystal microbalance (QCM) biosensor chips. Siyu is currently a postdoctoral researcher in the group of Prof. Andreas Walther at the Johannes Gutenberg University of Mainz (Germany). Her research mainly focused on the design and synthesis of functional DNA-based protocells to establish adaptive and interactive communication and system behaviors with biological cells and realize downstream applications.

Tsvetomir Ivanov is currently a PhD student in the group of Prof. Katharina Landfester at the Max Planck Institute for Polymer Research. He obtained his double master's degree in chemical engineering through a cooperation between the University of Chemical Technology and Metallurgy Sofia and Hamburg University of Technology in 2019. His thesis focused on the solute-dependent stability of GUVs. He is currently working on engineering vesicle-based artificial cells that mimic the structure and functions of living cells.

Thao P. Doan-Nguyen received her Ph.D. from the Vidyasirimedhi Institute of Science and Technology (Thailand) under the supervision of Prof. Daniel Crespy in 2022. She then joined the group of Prof. Katharina Landfester at the Max Planck Institute for Polymer Research (Germany) as a postdoctoral researcher, where she studied the formation of artificial cytoskeleton. She is currently a research fellow at the National Institute for Materials Science (Japan), working on artificial cell development.

Lucas Caire da Silva received his Ph.D. from the University of Florida in 2016, working on precision polyolefins and polymer dynamics with Prof. Kenneth Wagener. He then joined the group of Prof. Katharina Landfester at the MPIP as a postdoctoral researcher, focusing on nested nanoparticle-in-vesicle systems for hierarchical catalysis. From 2020 to 2023, Lucas led research on bioinspired cell-like systems at MPIP, developing multi-compartment microreactors and artificial organelles. As of 2023, he is an Assistant Professor in the Department of Chemistry at McGill University.

Jing Xie received her PhD under the supervision of Prof. Wilhelm Huck at Radboud University (Nijmegen, the Netherlands) in 2020. She then moved to the MPI for Medical Research as a postdoc fellow and collaborated with Prof. Joachim Spatz. In July 2022, she joined the Department of Biomedical Engineering, West China School of Basic Medical Sciences & Forensic Medicine, Sichuan University as a professor. Her research focuses on the design and synthesis of polymer-based hydrogels as artificial ECM for cell culture and medical applications.

Katharina Landfester received her PhD in 1995. After a postdoctoral stay at Lehigh University, she worked at the MPI of Colloids and Interfaces, heading the miniemulsion group. From 2003 to 2008 she was a full professor at the University of Ulm. She was appointed as one of the directors at MPIP in 2008. Her research focuses on the creation of functional colloids for new material and biomaterial applications. She has published more than 800 papers in international journals, 30 reviews and holds more than 50 patents.

Shoupeng Cao obtained his PhD in 2020 at the Eindhoven University of Technology with Prof. Jan C. M. van Hest, funded by the Marie Skłodowska-Curie Action ITN NANOMED program. He then joined Prof. Katharina Landfester's group as a postdoctoral fellow at the MPI for Polymer Research, In May 2022, Shoupeng was awarded the Humboldt Postdoctoral Fellowship, supporting his independent research on biomimetic materials with life-like features. From May 2024, he has been a principal investigator in the Department of Polymer Science and Engineering at Sichuan University.

machinery for biotechnology purposes, such as catalytic microreactors with tunable efficiency and selectivity.[18] In addition, the integration of adaptive and dynamic features allows synthetic condensates to form and dissolve in response to a variety of biological, chemical and physical cues.[19] This is of particular importance in the design of functional synthetic coacervate droplets with emerging applications in areas such as material science and biomedicine.

This minireview aims to discuss the up-to-date progress in the design and construction of synthetic coacervate-based biomimicry condensates. We will start with the general phase-separation behaviors towards engineering synthetic biomolecular condensates, including their rational and physicochemical control. The design of synthetic biomolecular condensates from a chemical and synthetic perspective will be highlighted. Instead, reconstitute condensates from biological components (e.g., fused in sarcoma (FUS) protein, heterogeneous nuclear ribonucleoprotein A1 (hnRNPA1), Tau protein) will not be included in this minireview, here we would like to refer to relevant research and reviews in this article for those interested.[20] We will then discuss the critical roles of synthetic condensates in biomimicry to replicate cellular organization and structural compartmentalization. The dynamics and life-like behaviors of synthetic condensates, as well as their phase-separation control strategies will then be illustrated. Given the vast array of available design strategies and control approaches over phase separation and biomimicry modeling in synthetic biomolecular condensates, we will focus on informative examples of different concepts rather than attempting to be comprehensive. Furthermore, as emerging synthetic coacervate droplets displayed unique microenvironments and merits as alternative paradigms in the catalytic and medical delivery fields, the potential utilities of synthetic condensates will also be discussed.

2. Formation and Biomimetic Features of Synthetic Biomolecular Condensates

2.1. Liquid-Liquid Phase Separation

Intracellular liquid-liquid phase separation behaviors occur when biomacromolecules such as proteins or nucleic acids undergo association via multiple, but weak interactions, reaching a critical threshold concentration.[21] This process favors biomolecule demixing from a single, homogeneous phase into two phases containing a highly concentrated, condensed phase surrounded by a diluted phase.[22] The biological phase-separation process is a highly dynamic and reversible process, which can be rapidly initiated or reversed in response to changes in cellular conditions, such as temperature, pH, ionic strength, or post-translational modifications (e.g., phosphorylation).[23] The assembly and disassembly of biomolecular condensates are crucial for cells to dynamically regulate their internal environment, which usually involves processes that require transient compartmentalization, such as stress responses, signal transduction, or the sequestration of specific molecules.[24] Via adapting this biological principle, synthetic (macro)molecules with a facile variation of molecular weight, chemical structures, architectures, charge density, and access to alternative functional groups can also undergo similar LLPS procedures.[25] The affinity interactions between synthetic (macro)molecules induce desolvation and phase separation, yielding macroscopically separated coacervate-based liquid droplets, usually in the micro-size range (1–100 μm).[26] The molecular interactions driving the LLPS and formation of synthetic condensates are very similar to those involved in biomolecular condensation, including electrostatic interactions, π–π stacking, hydrophobic interactions, cation-π interactions, and hydrogen bonding.[27] Generally, segregative or associative phase separation are two common types of interactions involved in the artificial LLPS, which usually result in two distinct liquid phases with each enriched in one type of molecules or one enriched phase surrounded with a diluted environment, respectively.[28] Due to the vast approaches and abundant strategies towards LLPS in synthetic materials, we here mainly focus on associative phase separations towards engineering synthetic biomolecular condensates. They are more relevant to reflect and mimic intracellular phase-separation behaviors. We would like to refer to other in-depth reviews related to segregative phase separation for those interested.[29] The associative phase separation between synthetic (macro)molecules is usually influenced by various biological (protein, nucleic acid, enzyme), chemical (composition, concentration, charge, chemical fuel, pH value, and reduction/-oxidation), and physical (temperature, light, osmotic pressure, shear force, surface tension) factors.[30] These factors have a strong impact on molecular interactions and changes in the environment, mediating dynamic assembly and disassembly of synthetic coacervate droplets.[31] The synthetic molecules undergoing LLPS commonly yield one-phased simple coacervates and complex coacervates, as well as multi-phased coacervates.[32] Simple coacervates are formed by a single type of molecule or polymer, while complex coacervates are LLPS results from two or more types of oppositely charged macromolecules, such as proteins and polyelectrolytes.[10c,32a,33] Synthetic coacervates generally display a membrane-less feature, while can also show surface membranization via interfacial engineering.[26a,34] They usually contain a relatively large amount of solvent in the same phase (50 %~90 % weight ratio) and are highly hydrated, displaying aqueous droplet features with coalescence behaviors.[10c] The membrane-less feature enables coacervate droplets to dynamically exchange with the surrounding environment and freely sequestrate functional solutes.[10b] Surface membranization renders synthetic coacervates with higher stability, potentially gated membrane transportation, and hierarchical organization features that more closely mimic integrated cells (Figure 1a).[34]

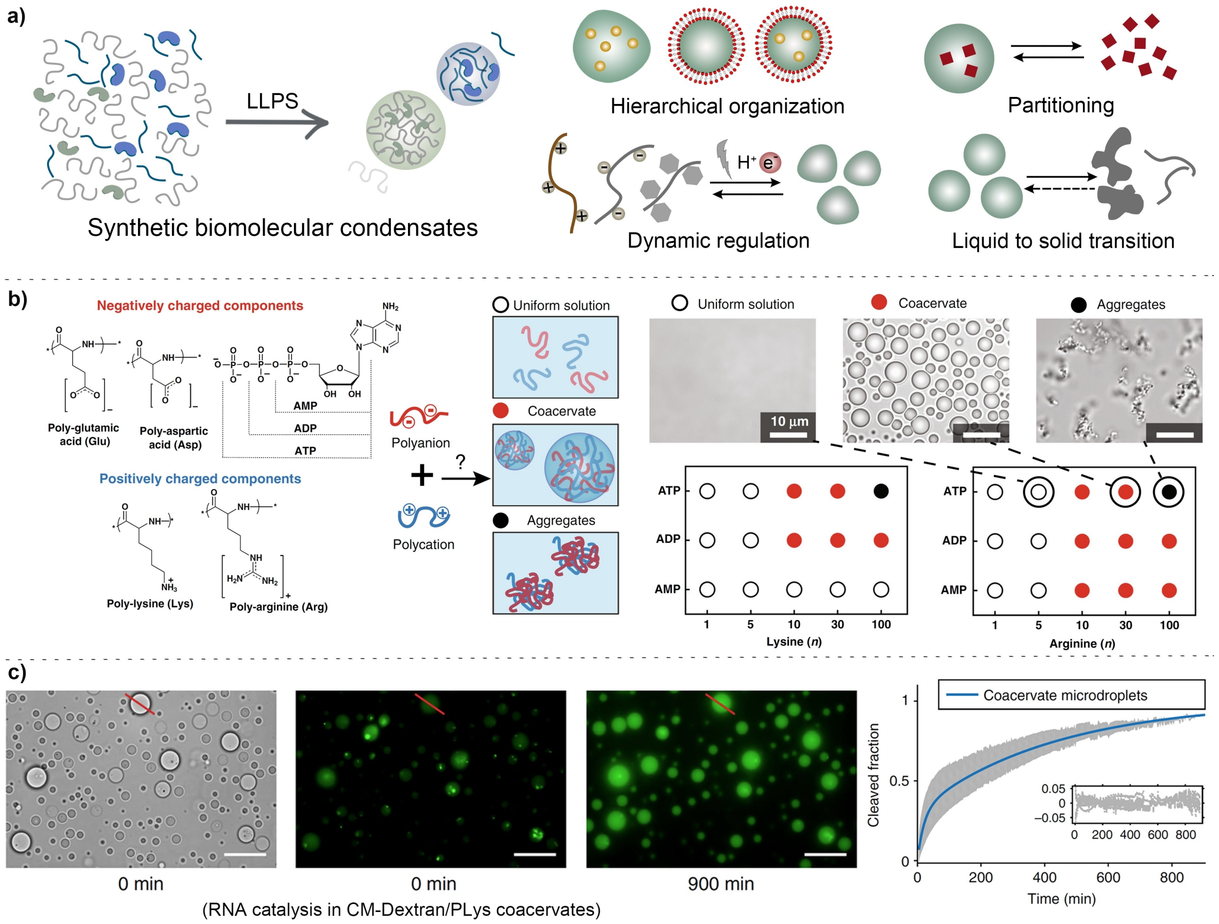

Figure 1. a) Schematic illustration of the LLPS procedure that induced (macro)molecules demixing into various types of condensates surrounded by a diluted environment, similar to the existence of various types of biomolecular condensates in living cells. The liquid droplets can show different features of structure organization and life-like behaviors. b) Coacervates between synthetic polymers and nucleotides are affected by the variations in charge and composition, which usually result in a transparent solution, coacervate droplets and aggregates. Reproduced from Ref. [25] with permission, Copyright 2020, Springer Nature. c) Left: coacervates from carboxymethyl dextran and polylysine for RNA catalysis (with hammerhead ribozyme and fluorescence resonance energy transfer (FRET) substrate), which showed enhanced emission (green: 6-carboxyfluorescein (FAM)) after prolonged incubation. Right: The increase in the fluorescence intensity of droplets indicated successful confined RNA catalysis. Reproduced from Ref. [38] with permission, Copyright 2018, Springer Nature.

2.2. Life-Like Structure and Organization

2.2.1. Membrane-Free Protocells

It is increasingly recognized that molecular assembly and the formation of protocells (i.e., simple synthetic cell-like structures designed to mimic the basic functions and features of living cells) are probably significantly important elements in early life, especially in the organization of prebiotic building blocks for biochemical reactions.[35] To understand the biological complexity, earlier researchers usually utilized lipid vesicles (i.e., liposomes) to replicate the intracellular compartmentalization and formation of protocells.[36] However, their diluted interior and the lack of membrane permeability control hinder their further development in modeling biological systems. Synthetic coacervates do not have those limitations and are more appealing biomimicry candidates because they have a dense, molecularly crowded liquid core that is a better mimic of the cytosol.[10b] They are usually formed via charge pairing between positively charged polymers (e.g., polylysine and polyarginine) and negatively charged species (e.g., carboxy-polymers, nucleoside phosphates, modified proteins, and various nuclear acids), resulting in the formation of typical complex coacervates.[13b,37] The Mann group is leading a pioneering role in the assembly and function of protocells. One widely used charge pair for complex coacervation is adenosine triphosphate (ATP) and polylysine (PLL), yielding micrometer-sized liquid-like droplets.[32a] They showed responsiveness to a variety of environmental cues such as ATPase, pH, and CO_2/N_2, enabling the reversible generation of coacervate droplets in a controlled manner. Highly charged coacervate droplets allow for the uptake, partition, and concentration of various active species from molecular photocatalyst to macromolecular enzymes. Complex coacervation between multivalent polyelectrolytes is strongly affected by factors including chemical composition, charge type, and charge density. The Keating group investigated a complex coacervate library comprising pairs of positively and negatively charged homopeptides (polyglutamic acid, polyaspatic acid, polylysine, polyarginine) with 1–100 residues and polyion pairs including adenosine mono-, di-, and triphosphate nucleotides. They found that charge type and density strongly impact the coacervation behaviors and the resulting membraneless compartments with short polyions showed a distinct internal microenvironment (local pH value, partitioning of ribonucleic acid (RNA)), and effect on RNA structure formation (Figure 1b).[25] Coacervates formed by shorter polyions have less dense and less uniformly distributed charges compared to those formed by longer polyions. It rendered shorter polyions-based coacervates to display more pronounced differences in apparent pH between the coacervate interior and the surrounding solution. Shorter polyions also allow RNA to more easily compete for binding sites with the coacervate's components, leading to higher RNA concentrations inside the droplets. Shorter polyions are less disruptive to RNA duplex formation and short-range secondary structures, while longer polyions more strongly interfere with both due to increased competition for binding sites. Coacervate droplets displayed a unique capacity to spatially localize and concentrate active molecules, enabling utility as a confined microreactor. This brings advantages for various biotechnology purposes such as accumulating ribozymes, RNA catalysis, and protein expression with tunable kinetics and improved efficiency, offering a mechanism for functional prebiotic compartmentalization in the origins of life (Figure 1c).[38]

2.2.2. Membrane-Free Organelles

Synthetic coacervate droplets, as typical membrane-less compartments, are considered viable tools for modeling intracellular membrane-less organelles, also known as, biomolecular condensates.[17d,39] They are specialized, membrane-free structures inside living cells that perform distinct vital functions such as protein synthesis and energy production.[5a] Coacervate droplets and biomolecular condensates share similar formation principles and biophysical features.[7b] Biomimicry concept and design make it feasible to integrate features of biological structure and organization with synthetic coacervates. This enables engineering integrated cytomimetic systems at an advanced level while being equipped with sophisticated functions. Recently, there has been a rising trend to assemble synthetic coacervates as membrane-less organelles and limit their LLPS in membrane-bound confinements (e.g., liposomes, polymersomes, and proteinosomes).[40] This is especially important to carefully tune and finely characterize the dynamics of LLPS in the initial state.[12b] Conventional LLPS in bulk conditions usually takes a very short time (i.e., seconds to minutes), and it is extremely difficult to track and control the LLPS process, as well as to compare their metastability and aging process with that in a confined environment. Limiting the LLPS in confinement increases the relative stability of synthetic coacervates, which are known to form adherent patterns on surfaces after prolonged incubation in bulk solutions.[41] In addition, it also allows the spatial location of functional machinery such as catalytic enzymes in the confinement.[42] The formation of synthetic coacervates as membrane-less organelles in a membrane-bound matrix also enables regulating the uptake of substrates/fuels selectively via membrane-gated transportation.[43] This is especially useful for pathway and kinetic control of biochemical reactions in coacervate-based organelles to a further advanced level. Representative examples are brought by the groups of Huck, Qiao, Tang, Dekker, and Landfester, in which LLPS between charged (macro)molecular species can be confined in membrane-bound compartments (Figure 2a/2b).[40a,42–44] This yields an artificial organelle within a membranized compartment with tunable membrane permeability, replicating key features of biological life such as multi-compartmentalization structure and hierarchical organization. These biomimetic systems enable the harvesting of functional biomacromolecules (e.g., DNA, proteins, and enzymes) and the recruitment of substrates through membrane transportation in a highly controlled and selective manner, yielding controlled microreactors with enhanced efficiencies.[43] This is an exciting way to construct life-like compartments to investigate complex metabolic reaction networks and embodied chemical computations. Future work should focus on enhancing molecular crowding, improving control over multi-phase separation and selective membrane permeability within the system to better replicate the highly organized and crowded intracellular spaces. Responsiveness to external stimuli for dynamic regulation of coacervate behavior and enabling more complex biochemical processes to occur should also be considered.

2.2.3. Membrane-Bound Integrated Synthetic Cells

The formation of sub-coacervates inside membrane-bound confinement (e.g., liposomes and polymersomes) is a viable engineering strategy for mimicking organelle structures, hierarchical organizations, and membrane features observed in living cells.[40b,45] However, a major limitation is that the interiors of these confined compartments often remain largely diluted, failing to achieve molecular crowding, one of the hallmarks in living cells.[46] This dilution may reduce the concentration of reactants and biomolecules, hindering efficient biochemical interactions and limiting the system's ability to mimic the highly organized and dense environment of the cytoplasm. One example is the concentration of enzymes within cellular organelles, which ensures efficient metabolic processes. In synthetic analogs, the lack of a fully crowded interior can slow down or impair reaction kinetics, reducing the system's functionality. Another alternative approach to replicating the interior crowding and hierarchical features of living cells is to generate an interfacial membrane on the surface of synthetic coacervates.[26a,34] This is an important step in engineering coacervate droplets towards integrated protocells, containing a fully molecular crowded interior enclosed with a membrane.[46b] Surface self-assembly of phospholipids and polymers has been presented as a practical strategy for interfacial reconfiguration and

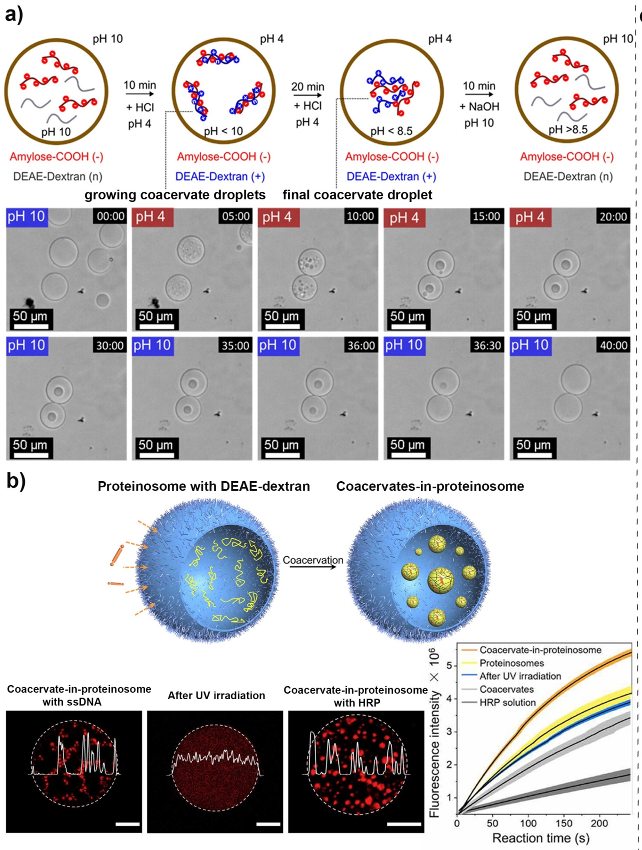

Figure 2. a) pH-induced formation of coacervate organelles (from carboxy modified amylose (amylose-COOH) and diethylaminoethyl-dextran (DEAE-dextran)) inside giant polymersomes. The coacervate formation is dependent on environmental pH, which initially formed numerous small droplets at acid pH and then fused into a single droplet. Increasing the solution pH can degrade the coacervates back into the dispersed state. Reproduced from Ref. [44] with permission, Copyright 2023, American Chemical Society. b) The diffusion of trans-AzoGlu$_2$ (i.e., 4,4′-glutamic acid azobenzene) into proteinosomes enables complex coacervation with DEAE-Dextran in the confinement. The coacervates displayed responsiveness to UV light, which allowed for them to reversibly capture ssDNA (TAMRA labeled). When applied in enzymatic reactions such as Amplex red assay, the coacervate-in-proteinosome structure compared with other controls showed an enhanced efficiency. Reproduced from Ref. [42] with permission, Copyright 2021, AAAS. c) Formation of membrane-bound synthetic coacervates via interfacial charge interactions. Reproduced from Ref. [47b] with permission, Copyright 2017, American Chemical Society. d) Lipids assembly on the surface of complex coacervates (from DEAE-dextran and DNA) yields membrane-bound coacervates as integrated cell mimics. This membrane-enclosed giant coacervate vesicles (i.e., GCV) displayed enhanced Ribozyme activity (i.e., Mg^{2+}-triggered ribozyme-mediated strand cleavage reaction) compared with the bulk situations (i.e., PBS), as shown in the plotted profile. Reproduced from Ref. [49a] with permission, Copyright 2021, American Chemical Society.

membrane formation of coacervates, taking advantage of the optimized interfacial tension and interface width.[47] The integrated biomimicry design and having a membrane around coacervates can significantly enhance their functionality by providing several important advantages. Surface membranes provide structural stability of coacervates, helping them resist coalescence or fusion, which is a common issue in membrane-free systems.[47b] This stabilization enables the preservation of small, distinct droplets that can carry out specialized functions over extended periods. The surface membrane also serves as a protective barrier, helping to maintain the integrity of the coacervate structure and preventing the uncontrolled exchange of materials with the surrounding environment. In addition, the membrane render key features for the coacervates such as controlled permeability.[17c,19e] This allows the selective uptake and exchange of substrates/fuels from the surrounding environment, enabling better control over the internal environment and regulating the movement of ions, nutrients, or signaling molecules. Membrane structure is essential for compartmentalized reactions, allowing for the isolation of biochemical processes within a confined space, that resemble organelles in a living cell.[47a] This may also enable the coacervate to carry out multiple functions (catalytic reactions) simultaneously in different compartments with pathway and kinetic control while keeping them spatially organized. Furthermore, surface membranes can also show responsiveness to environmental triggers or cues, which allows for active communication with the external environment, signal processing, or targeted delivery of therapeutic agents.[19e] However, polyelectrolyte-based complex coacervates usually show limited biocompatibility or even toxicity when cultured with cells due to their highly charged nature.[48] Surface membranization with biocompatible shielding groups, such as PEGylated polymers, enhances the biocompatibility criteria of synthetic condensed hydrates for biologically relevant applications. In addition, it is also feasible for membrane-bound coacervates to establish a non-equilibrium condition at the coacervate/water interface, which is usually required for modeling cytomimetic features to a further advanced level.[26a] The groups of Keating, van Hest, and Mann introduced pioneer concepts in the formation of integrated synthetic cells using charged lipids or amphiphilic terpolymer with a short-charged chain as membrane components for stabilizing polyelectrolyte-based coacervates (Figure 2c/2d).[47b,49] Via adapting similar principles and charge pairing interactions, modified proteins, colloid nanocapsules, and biological cellular wall fragments have also been proven as effective elements for the surface stabilization and membrane formation of highly charged polyelectrolyte-based droplets, which can render key features such as recognition, specific binding, and bacteria capture.[50] Alternative strategies including interfacial nanoparticle assembly and crosslinking were also applied in the interfacial stabilization and membranization of coacervate droplets while rending emerging properties and applications.[17c,19e] Future work on membrane-bound integrated synthetic cells should focus on optimizing membrane stability, permeability, and responsiveness to environmental stimuli, while integrating active biochemical processes and spatially organized molecular crowding to better replicate natural cellular environments. Advancing scalable production and improving biocompatibility will also be critical for enhancing their potential in biomedical applications.

2.2.4. Multi-Phase Features of Synthetic Biomolecular Condensates

Many biological organelles such as nucleoli and stress granules are actually multi-phase condensates with dynamic formation and hierarchical structures, which contain distinct, coexisting phases within a single droplet-like structure.[23a,51] Synthetic coacervates can also show multi-phase separation behaviors, which are suggested to provide crucial insights into the biological principles, molecular interactions, and chemical grammars underlying the formation and emergent behaviors of multi-phase organelles.[32c,52] They are usually constructed from relatively complex components that undergo multi-phase-separating behaviors due to distinct molecular interactions.[13b] These interactions include hydrogen bonding, ionic interactions, van der Waals forces, and hydrophobic effects.[10c,21a] For example, hydrogen bonds can form between molecules with complementary donor and acceptor groups, promoting the selective partitioning of components within a specific region.[53] Ionic interactions occur between charged species, such as oppositely charged polyelectrolytes, leading to the formation of distinct, charged domains.[32c] These molecular interactions influence the structure of coacervates by determining how different molecules are distributed within the system. Strong ionic interactions between oppositely charged polymers may result in more rigid, viscous regions, while weaker hydrogen bonding could lead to more fluid, dynamic areas.[25] This variability in local physical properties—such as viscosity and charge—creates multiple phases within a single coacervate, allowing for the selective partitioning of biomolecules into distinct microenvironments.[54] This makes it viable to show different local features and specialized microenvironments (i.e., charge, fluidity, viscosity) in distinct compartments to selectively partition active biomolecules in physically separated regions.[55] The spatial locations and distributions of functional biomolecules in the multi-phase coacervates are of critical importance to organize and regulate complex biochemical reactions in a controlled manner.[56] This makes it feasible to facilitate multi-complex pathways and incompatible reactions, increasing the diversity of reaction networks and realizing proper biotechnological functions.[57] Several strategies have been proposed to shed light on the formation of multiphase coacervates through tailoring key factors affecting LLPS including chemical components, critical salt concentrations, and interfacial tension.[32c,54] For instance, Spruijt and co-workers found that if the interfacial tension of multiphase-coacervate is lower compared with that of sing-phase coacervates, it would favor the formation of a multilayer structure.[32c] And different critical salt concentrations of coacervates induced distinct densities which are essential to remain the demixing statues in a multiphase droplet. Besides that, the critical salt concentration also induced an effect in the spatial-distribution of different phases in the multiphase droplets. They noticed that the coacervate phase with the highest critical salt concentration, because of higher (charge) density and lower water content, usually located at the center of the multiphase coacervate. The dynamics of multiphase assembly can also be controlled, as introduced by Elbaum-Garfinkle and co-workers, who exploited different interactions between lysine and arginine residues with nucleotides to tailor multiphase assembly. When mixed with mono/polynucleotides, the droplets of polyarginine displayed approximately 100-fold greater viscosity than comparable lysine droplets, due to the ability to form π–π interactions between arginine molecules. The difference in amino acid level in the mixture system induced the formation of coexisting immiscible phases with tunable formation kinetics, which was further utilized for the triggered release of droplet components in a controlled manner (Figure 3a).[58]

Keating and co-workers further presented the formation of multi-phased droplets via manipulating the chemical components (containing arginine, R10; lysine, K10; or aspartic acid, D10) in the LLPS, which displayed different interfacial tensions and viscosities in the adjacent phase. A higher peptide concentration in a phase led to lower water content and higher viscosity. This increased viscosity made the inner phase less fluid and slowed the fusion of droplets in coalescence experiments (confirmed by fluorescence recovery after photobleaching (FRAP) experiments). Simultaneously, the difference in peptide concentration between phases created an interfacial tension; a greater difference (e.g., between the inner and outer phases) resulted in a stronger interfacial tension. The core–shell morphology observed in the multiphase droplets arose from this higher interfacial tension between the inner phase and the surrounding dilute phase. Introducing of coexisting phase

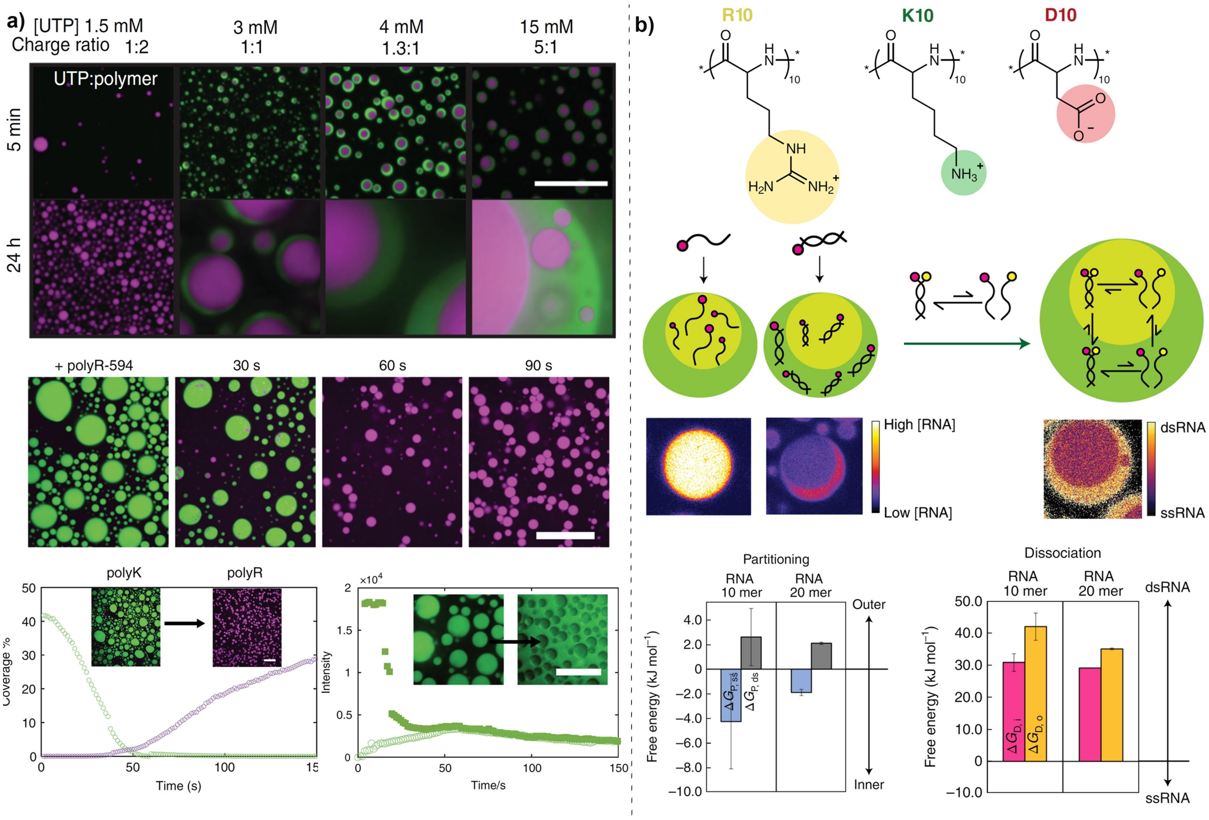

Figure 3. a) Top: Complexation of UTP (uridine-5'-triphosphate trisodium salt, from 1.5 mM to 15 mM) with polylysine (polyK, green-labeled) and polyarginine (polyR, purple labeled) (polyK:polyR 50:50 mixtures) displayed multiphase coacervation. Middle: the addition of polyR50 (labeled with dylight594 (purple)) displaced the polyK (fluorescein isothiocyanate (FITC)-labeled (green)) coacervation with UTP. Down left: A complete condensate inversion was observed with polyK droplets being entirely replaced by polyR upon mixing of polyR into polyK-UTP condensates. Down right: The intensity of FITC-polyK inside polyK droplets decreased over time and the outside fluorescent intensity increased due to the condensate inversion. Reproduced from Ref. [58] with permission, Copyright 2020, Springer Nature. b) Top: Chemical structure of R10, K10, and D10. Middle: Complexation of polyaspartic acid with polylysine and polyarginine yielded multiphase coacervates, which showed distinct partition behavior of RNAs and RNA destabilization efficiency. Down left: Difference in the Gibbs free energy in the partitioning of ssRNA and dsRNA from outer to inner coacervate phases; Down right: Difference in the Gibbs free energy in the dissociation of dsRNA into ssRNA in inner and outer droplets. Reproduced from Ref. [54] with permission, Copyright 2022, Springer Nature.

not only produces distinct chemical environments for concentrating guest biomolecules to different extents but also gives rise to new thermodynamic equilibrium that significantly influences spatial RNA partitioning and duplex dissociation (Figure 3b).[54] Future work should focus on establishing sequence-level changes that influence dynamic behaviors, material properties, colloidal stability, and function of the multiphase condensates, in order to build general design rules to engineer condensates with specific features and behaviors.

3. Life-Like Behaviors

3.1. Growth and Division

Intracellular biochemical reactions and molecular networks provide energy and fuels for the growth, replication, and division of biological cells, which are the fundamental processes for sustainable cell development. However, it is extremely challenging to elucidate the detailed mechanisms and pathways for biological growth and division. Synthetic analogs that mimic the biological complexity and replicate these dynamic behaviors contribute to unraveling the fundamental insights, as well as showcasing new opportunities to study life-like behaviors.[59] Coacervate droplets are widely observed to undergo passive growth into thermodynamically favorable bigger droplets, via coalescence and fusion, or absorbing surrounding materials, due to diffusion and minimization of surface energy.[26a] Synthetic condensates can also undergo biochemical processes that induce swelling and fusion with active control, mimicking the chemically transduced process found in cell adaptation.[59a] The Walther group is leading a pioneering role in the biomimetic engineering of DNA protocells with structural morphogenesis and downstream applications via chemical signal processing. DNA-based condensates after surface membranization can harbor artificial metalloenzyme and olefin metathesis reactions inside the DNA condensates, promoting morphogenetic response (i.e., swell and fusion) of the protocells (Figure 4a).[60] Apart from growth, division and fission are also essential for evolution and for the

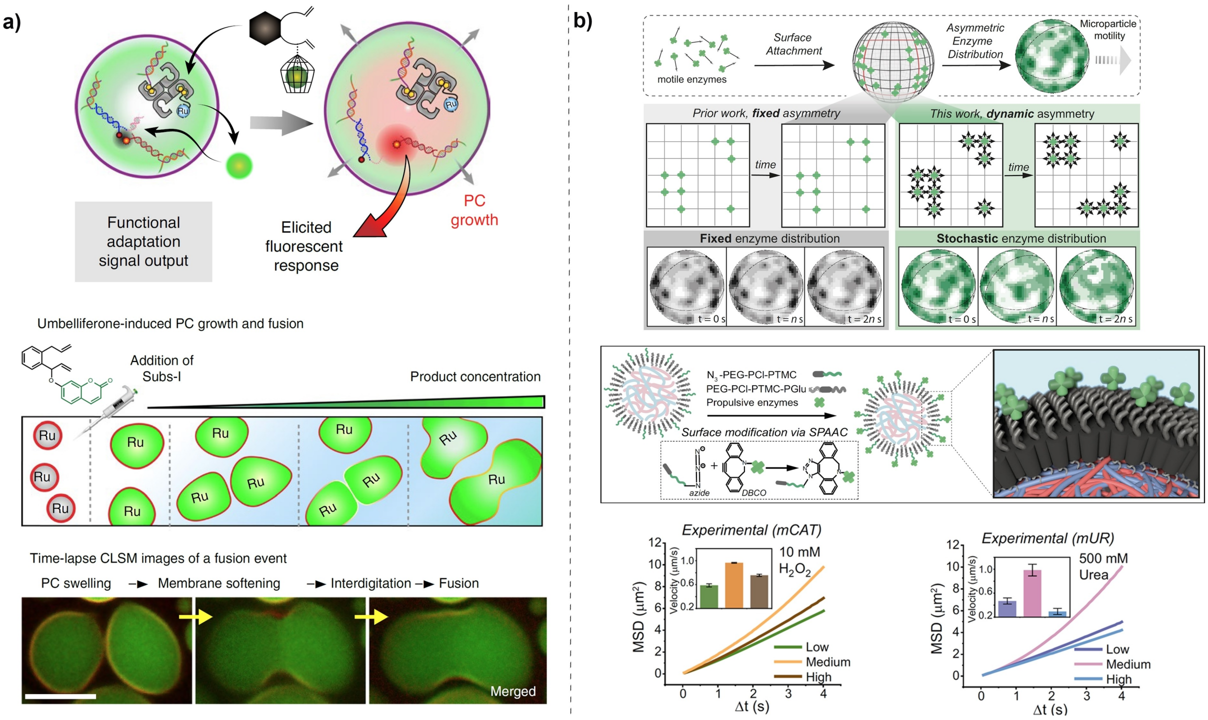

Figure 4. a) Top: DNA coacervate-based protocells displayed growth and fusion behaviors. The bio-orthogonal reaction within the coacervates induced a decaging process that induced swelling of the protocells, which also triggered a secondary fluorescence output. Middle: Scheme illustration of a decaging reaction that induced swell behavior of the protocells. Down: Swelling of the protocells induced fusion of the DNA-based protocells. Reproduced from Ref. [60] with permission, Copyright 2020, Springer Nature. b) Top: Scheme illustration of the design philosophy to translate a stochastic process into autonomous motion in an artificial system. Middle: Stochastic engineering is realized via attaching an active enzyme (catalase or urease) on the surface of polymer-stabilized complex coacervates. Down: In the presence of fuels (H_2O_2 or Urea), the enzyme-immobilized coacervates showed enhanced motion behaviors. Reproduced from Ref. [65] with permission, Copyright 2021, Springer Nature.

production of offspring in living systems and important for biomimicry systems.[59b] The division of coacervate droplets contributes to transferring molecular information to succeeding daughter droplets. This allows the passing of evolutionary merits to the next generations. However, it is very difficult for coacervates to divide, since overcoming the tendency of coacervate droplets to relax to a spherical shape is challenging due to minimized surface tension of spherical droplets.[59a] The Tang group plays a strikingly important role in coping with such an issue. They introduced a non-equilibrium condition inside rock pores for manipulating the dynamic behaviors of coacervate droplets. The gas bubbles inside heated rock pores perturbed the coacervate protocell distribution, which drives the accumulation, fusion, maintenance, and fission of coacervate droplets.[61] Future work about exploring active, energy-driven mechanisms that can more closely mimic cellular processes like autonomous division and adaptation to environmental cues will be crucial. The integration of synthetic systems with external stimuli could allow for precise manipulation of coacervate dynamics, providing deeper insights into life-like behaviors.

3.2. Motility

Cell motility is essential for their healthy growth via adaptation and interaction with surroundings while avoiding damage. It also can bring important merits to living systems such as wound healing, immune response, and embryonic development. Integration of motility in the design of synthetic materials via adapting biological principles can give rise to complex behaviors and proper functions. It enables precisely controlled migration of synthetic compartments to a spatial localized position and collective interactions.[62] Previous research on the motility of synthetic compartments mainly utilized liposome-based systems, which displayed directional movement via for instance light-guided adhesion, burnt-bridge mechanism, or buoyance-induced motion.[63] Synthetic coacervates with molecular crowded interiors and a denser feature utilized alternative mechanisms such as enzyme reaction and chemotaxis to drive their motion.[64] The van Hest group leads a pioneering role in the design and construction of synthetic condensates with active motility, via adapting similar principles and concepts for enzyme-powered nanomotors. It is generally realized via chemical conjugation of an active enzyme (e.g., urease and catalase) on the surface of membrane-bound polyelectrolyte-based coacervate droplets. The surface enzyme modification resulted in a transient and asymmetric configuration of propulsive units, which induced active motility to coacervate droplets in the presence of fuels (i.e., H_2O_2 and urea) (Figure 4b).[65] In addition, the active motion of synthetic coacervates was also realized in lipid-based confinement, mimicking the motion of biomolecular condensates in confinement.[17b] These works represented conceptual advances in the design and construction of synthetic systems with life-like behaviors and provided versatile approaches to understanding the fundamental behaviors of active matter. Future work should focus on enhancing the complexity and versatility of dynamic systems with active motility to better emulate the behaviors of living cells, which includes exploring the integration of multiple motility mechanisms within a single synthetic compartment, allowing for adaptive responses to various environmental stimuli. Additionally, incorporating feedback loops that enable synthetic systems to sense and respond to their surroundings could lead to more sophisticated behaviors, such as swarm intelligence or cooperative movement.

4. Dynamic Control

Biomolecular condensates can be facilely controlled and dynamically regulated by a series of biochemical factors and chemical-physical approaches such as environmental changes and post-translational modifications.[6a] This enables them to reversible assembly and disassembly in response to specific triggers and external stimuli, such as the stress granule formation from amyotrophic lateral sclerosis (ALS)-related RNA-binding proteins (RBPs) hn-RNPA1 in response to environmental stresses.[24b] The dynamic regulation of intracellular condensates is of great importance in a variety of biochemical processes, such as cellular metabolism, enzyme reaction, genetic information signaling, and transcription.[5a] In light of this, engineering synthetic coacervates with dynamic control is of great value to directly establish relationships between condensation behaviors and stimulation while eliminating unpredictable biochemical effects.[28a,66] Synthetic coacervates that displayed life-like adaptive behaviors would be very helpful in elucidating the dynamic features of biomolecular condensates from a molecular level. It also enables the engineering of advanced synthetic materials for diverse potential bio-related applications.

4.1. pH Value

LLPS of synthetic coacervates are usually driven by electrostatic attraction between charged (macro)molecules and polyelectrolytes, which are highly sensitive to environmental pH value.[42] Representative examples of coacervation pairs that are sensitive to pH value include ATP/polylysine, ATP/polyallylamine, and DEAE-dextran/carboxy-dextran/enzyme, in which pH change modulates the strength and nature of electrostatic attractions and repulsions.[40b,42] Environmental pH-induced modulation is a straightforward, easily accessible, and widely utilized approach toward controlling the phase-separation behaviors of synthetic coacervates, including the formation, stability, and dissolution of the droplets.[12b,19b, 67] Due to the vast presence of pH-responsive moieties (e.g., amino, carboxy, tertiary amine, and phosphate groups), pH modulation generally requires minimal chemical additives that can be facilely realized through various approaches (e.g., the addition of acid/base, enzyme-coupled pH change, CO_2/N_2 gas bubbling).[13b,32a]

In addition, pH changes in the environment can be easily reversed, which allows for fine-tuning the coacervation process in a highly controlled and dynamic manner.[67] This is of critical importance for applications where coacervates need to be transformed in different states for specific purposes. A typical example is illustrated by Tang and coauthors, in which synthetic coacervate-based organelles were integrated inside membrane-bound liposomes via confined pH-induced coacervation (Figure 5a).[67] Polylysine and ATP were utilized as the pairs for coacervates, which displayed coacervation and activity (i.e., concentrating enzymes and substrates) below pH 9, but showed inert activity above pH 11 due to the deprotonation of PLL. The pH-induced coacervation inside a confinement not only represented a dynamic formation of a hierarchical synthetic cell model but also activated dormant enzyme reactions (for the production of nicotinamide adenine dinucleotide reduced (NADH)) by increasing the local concentration within the coacervate droplets. Synthetic coacervates with pH-responsiveness are a highly dynamic area of research with broad potential applications in fields such as drug delivery, materials science, and environmental sensing.

4.2. Reduction and Oxidation

The intracellular reduction/oxidation (redox) balance is of critical importance for the healthy and proper function of living cells including ATP production, cellular respiration, avoiding oxidative damage, signal transduction, and protein function.[68] This is also crucial for biomolecular condensates to organize cellular biochemistry. Different redox states can influence their formation and stability through oxidation-sensitive interactions among proteins and nucleic acids, which also control key functions and features.[2b] This biological principle and molecular mechanism were also utilized in the engineering of synthetic coacervates with dynamic formation.[32b] It offers an alternative paradigm to mimic cellular processes including the impact of redox reactions in molecular interactions and compartmentalization. Manipulating the redox state in synthetic coacervates is also a viable tool to control their microenvironment to mediate biochemical reactions and the formation of complex structures. A variety of reduction or oxidation-responsive groups including thioether, disulfide bond, nicotinamide adenine dinucleotide phosphate ($NADP^+$), and ruthenium (II) complex have been integrated into molecular or polymeric building blocks for LLPS.[13a,32b,69] Upon subjecting to a reductive or oxidative environment, these responsive groups usually underwent chemical transformations that turned the hydrophobicity/hydrophilicity of the coacervate

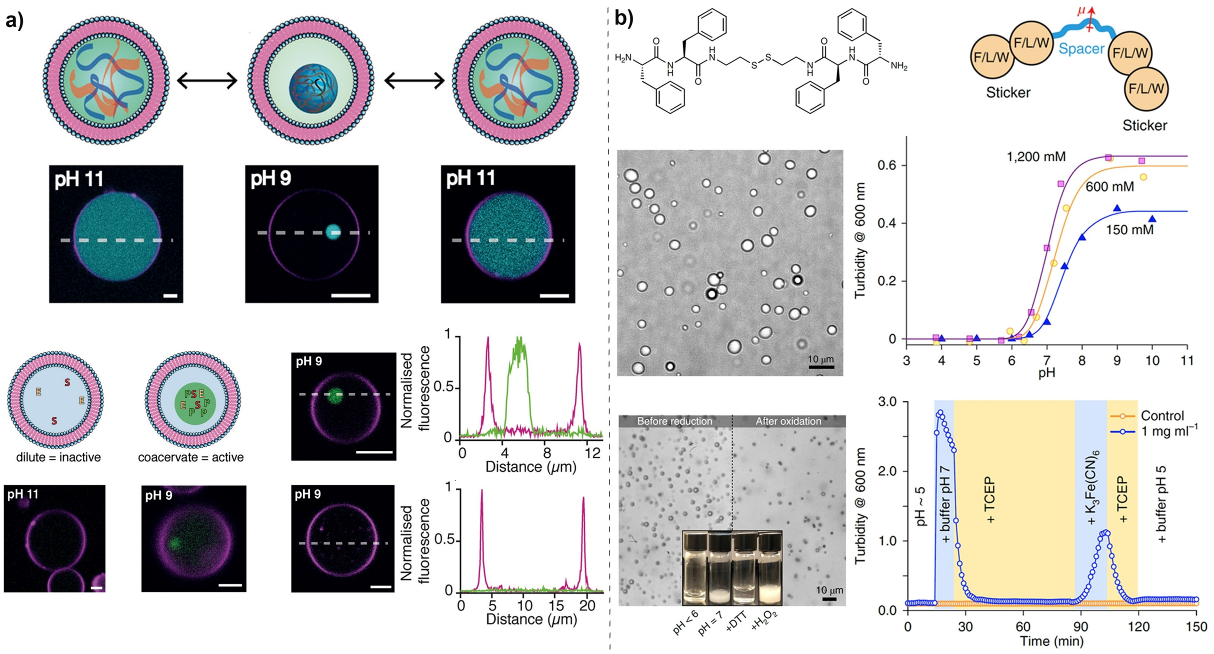

Figure 5. a) Top: pH-triggered reversible coacervation between PLL and ATP inside liposomes, which displayed coacervation and activity below pH 9, but showed dispersed state and inert activity above pH 11 due to the deprotonation of PLL. Down: The pH-induced coacervation inside confinement activated dormant enzyme reactions (for NADH production) by increasing the local concentration within the coacervate droplets. Reproduced from Ref. [67] with permission, Copyright 2020, Wiley. b) Top: the design of peptide coacervates based on a sticker-spacer structure. Middle: The peptide formed coacervates at pH above 7, in which the presence of high concentrations of NaCl even induced an increase in the solution turbidity. Down: the peptide coacervates showed responsiveness and reversible phase-separation upon reduction and oxidation conditions, revealed by both microscopy and turbidity studies. Reproduced from Ref. [33] with permission, Copyright 2022, Springer Nature.

system. This usually leads to a triggered disassembly of the coacervates, which could be reversed under opposite conditions. Spruijt and co-workers designed a series of amphiphilic aromatic dipeptides integrated with a disulfide linker, which initially displayed a pH-induced coacervation into micro-sized droplets (Figure 5b).[33] The introduction of tris(2-carboxyethyl)phosphine (TCEP, 19 mM) led to the cleavage of the disulfide bond, thereby dissolving the peptides (1 $mg\,mL^{-1}$, ~1.3 mM). The addition of $K_3Fe(CN)_6$ (45 mM final concentration, >2 times the TCEP concentration) quenched the reductive condition and produced an oxidative environment. This contributed to the restoration of the appearance of coacervate droplets. Synthetic coacervates that can utilize biological principles offer insights into cellular processes and have potential applications in biotechnology, where redox-sensitive systems can be exploited for innovative solutions.

4.3. Enzyme

Regulation of biomolecular condensates via enzymatic pathways is an intriguing area of study due to their prevalent involvement in the formation, dissolution, and function of these condensates.[6b] For instance, kinases and phosphatases, that add or remove phosphate groups, alter the properties of proteins (e.g., charge, solubility), which can selectively promote or inhibit associated phase-separation behaviors.[70] This is of critical importance for the function of biomolecular condensates from sequestering molecules to organizing biochemical reactions. Adapting biological principle-inspired regulation and control of synthetic coacervates in a biomimicry manner is an emerging topic in the field of synthetic biology.[71] A representative example is the pyruvate kinase-catalyzed ATP formation via conversion of adenosine diphosphate (ADP) in the presence of a chemical fuel (i.e., phosphoenol pyruvate), which allows followed LLPS with a cationic fluorescent protein, K72 (72 repeat units of the pentapeptide VPGKG) (Figure 6a).[72] This led to the formation of active droplets with controlled dynamics. The continuous production of ATP and the local concentration increase inside the droplets resulted in the recruitment of more protein, leading to droplet growth. Enzymatic regulation is also a facile approach to control the lifetime of synthetic coacervates in bulk solutions and confinement, mimicking the adaptive formation of biological condensates in cells. To demonstrate coacervation with dynamic and biomimicry control, Cao et al. demonstrated the formation of adaptive synthetic coacervates (with PLL and ATP) inside a giant polymersome system.[43] The presence of co-encapsulated alkaline phosphatase did not impact the initial coacervation but degraded ATP and dissolved the coacervates after prolonged incubation. This resulted in a precisely controlled lifetime of confined synthetic coacervates from minutes to hours. Enzyme-responsive synthetic coacervates is an emerging area of research that leverages the dynamic and responsive nature of coacervates in combination with the specificity and catalytic efficiency of enzymes. The future

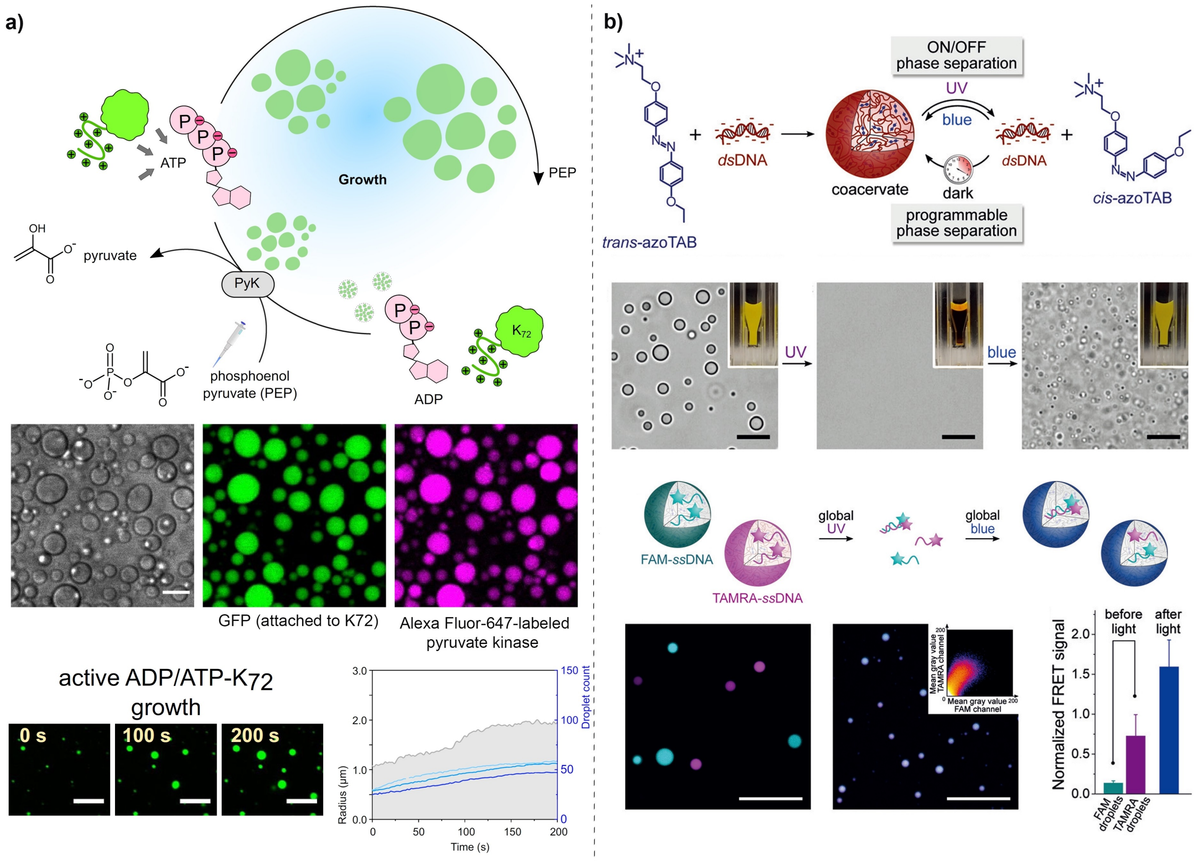

Figure 6. a) Top: Scheme illustration of enzyme-induced formation of active coacervate droplets by the catalytic conversion of ADP to ATP, enabling LLPS with ATP-K72. The local increase in the amount of ATP inside the droplets causes the recruitment of more protein, resulting in the growth of droplets. Middle: ATP-K_{72} droplets (green labeled) containing Alexa Fluor-647-labeled pyruvate kinase (purple labeled). Down left: the size of the droplet gradually increased with prolonged incubation. Down right: during the active formation of coacervate droplets, the size (black curve) and count (blue curves) of the droplets both increased. Reproduced from Ref. [72] with permission, Copyright 2021, Springer Nature. b) Top: Scheme illustration of light-responsive coacervates via LLPS between trans-azoTAB and DNA. Middle: Microscopy images showed that the DNA-coacervates disassembled after UV light irradiation, but re-generated after visible light irradiation. Down: The light-responsiveness of DNA-coacervates allowed for trafficking guest molecules between different populations of coacervates (FAM-ssDNA is cyan colored and TAMRA-ssRNA is magenta colored). After sequential UV-then-blue light irradiation, an increased FRET signal in droplets was observed. Reproduced from Ref. [73] with permission, Copyright 2019, Wiley.

research of enzyme-responsive synthetic coacervates is poised to develop smart, responsive materials with a wide range of applications.

4.4. Light

As a simple approach to realize precise control and spatiotemporal modulation, light demonstrated a powerful ability to mediate phase-separation and property control of artificial coacervate droplets.[10b,19e,66] This is valuable for studying dynamic processes and developing responsive materials. Photo-irradiation usually either affects the affinity interactions between the photo-responsive species and surrounding associated (macro)molecules or is utilized as energy input (e.g., producing heat or reactive oxygen species (ROS)) that can impact the properties of the resultant coacervates. The facilely tunable wavelength, laser intensity, and irradiation periods in the light control allow for reversible induction or dissolution, changes in fluidity and interfacial features of the condensates in a highly controlled manner.[19d,e,42] They are typically achieved through the incorporation of photo-responsive modules that alter their properties (mainly hydrophilicity and charge) upon exposure to specific wavelengths of light. A representative example is the use of charged azobenzene molecular switches, which are widely utilized in the construction of light-responsive coacervates. When a trans-azobenzenetrimethylammonium bromide (trans-azoTAB) is mixed with double-stranded DNA, liquid-like coacervate microdroplets are formed via attractive electrostatic interactions (Figure 6b).[73] These coacervates can be disassembled and reassembled upon UV and blue light irradiation within a few seconds, due to light-induced conformation change of trans-azoTAB and altered interactions with DNA. This mechanism further enabled the light-activated trafficking of guest molecules between different populations of coacervate droplets. Light-actuation mediated regulating pathways were also exploited for signaling activation and membrane-gated transportation, which is useful for trigged molecular communication and adaptive information processing.[43] This paves the way to build and engineer life-like colloidal systems that are capable of modulating behaviors with precise spatial and temporal control, enabling innovative solutions in biotechnology, materials science, and medicine.

In addition to pH, redox conditions, enzymes and light which have been usually utilized in the control of liquid-liquid phase separation, ions and temperature have also emerged as important factors for regulating the formation and activities of synthetic coacervates. Ions can influence coacervate formation and stability by altering electrostatic interactions and the ionic strength of the environment, leading to controlled assembly or disassembly of coacervates.[74] Temperature also plays a crucial role by affecting the phase behavior (increase or decrease of hydration or solvation) and viscosity of coacervates, enabling temperature-sensitive regulation of coacervate activity, such as reversible formation or molecular encapsulation and release.[75] These stimuli provide additional tools for fine-tuning the dynamic properties and functional behaviors of coacervates, expanding their potential in biomimicry, biomedical and material science applications.

4.5. Out-of-Equilibrium Features

Life is heavily involved with dynamic and out-of-equilibrium behaviors, with continuous consumption of fuels (e.g., glucose, fatty acids, amino acid) and production of energy molecules and products (e.g., ATP, NADH, chemical energy, protein gradient) to sustain survival and evolution. This is typically reflected in biomolecular condensates that are actively regulated by complex biochemical reactions, crucial for organizing various cellular processes and behaviors in a highly controlled manner.[2b,5a] Considering the cellular complexity, engineering out-of-equilibrium features in synthetic condensates would be highly valuable. This is crucial for fundamentally understanding the molecular mechanisms and biophysical principles underlying intracellular condensation behaviors and their dynamic and adaptive behaviors.[9a] It also enables synthetic coacervates to exhibit complex behaviors that can be finely tuned for various functions. Out-of-equilibrium features in the synthetic coacervate often arise from continuous input of fuels and the ability to respond to environmental changes. The Boekhoven group introduced the early concept of integrating living features with synthetic materials such as peptide coacervates. Usually, a C-terminal aspartic acid carrying a −2 charge was incorporated in the design of peptides that have 3 guanidine groups, which initially is not capable of forming complexation with negatively charged species. The addition of 1-ethyl-3-carbodiimide hydrochloride (EDC) converts an aspartate-based C-terminus into its corresponding acid anhydride, increasing the net charge of the peptides and induced coacervation with negatively charged species including polystyrenesulfonate and RNAs (Figure 7a).[30c,76] The following hydrolysis of the anhydride reverted the activation, reducing the complexation and degrading the coacervates with a tunable lifetime. DNA-based synthetic coacervates also can display life-like dynamic features. The Walther group demonstrated the formation of functional all-DNA coacervates via transient, multivalency-driven LLPS of sequence-defined functionalized nucleic acid polymers (Figure 7b).[77] The DNA coacervates were formed with a fuel-drive process with tunable dynamics, in which the presence of ATP as a fuel drove the LLPS, but the coacervates disappeared once the ATP was consumed. The bioinspired behaviors and conceptual advances are valuable for elucidating the biophysical principles and understanding the dynamics of living systems.

5. Emerging Applications of Synthetic Coacervates

5.1. Catalytic Compartments

Biomolecular condensates play a critical role in cellular organization by sequestering and concentrating biomolecular cues, thereby hosting a variety of complex biochemical reactions necessary for supporting vital cellular processes such as gene expression and DNA replication.[78] Via adapting biological principles, synthetic coacervates have emerged as a powerful candidate to create catalytic compartments that can mimic the dynamic, compartmentalized, and functional features of biological systems.[18a] Coacervate droplets are usually utilized as compartments for enhancing enzymatic reactions because complex coacervates are usually highly charged which enables them to sequestrate biological proteins and enzymes via charge affinity.[11c,42,47] Recent findings suggest that synthetic coacervates can also create a unique internal or interfacial microenvironment to mediate chemistry reactions in aqueous buffers, that were usually only active in organic solvents.[17a,33] This is because the microenvironment inside the coacervates can not only be designed with affinity to hydrophilic species but also can be tailored to partition hydrophobic molecules (like micellar environment) for chemical reactions. The Silva group recently found that minimal peptide coacervates boosted the activity of a hydrophobic transition metal-based catalyst (i.e., a ruthenium complex), mediating biorthogonal decaging reactions and producing fluorescent products (Figure 8a).[50b] This is because the peptide coacervates as a crowded compartment displayed affinity towards both the hydrophobic substrates and catalyst, concentrating them inside the compartments and enhancing their reaction rates in aqueous environments. The peptide coacervates carrying a metal-based catalyst were incorporated as active artificial organelles in cells and triggered an internal non-biological chemical reaction. Catalytic reactions inside coacervates can also be used to create biomimetic cytoskeleton structures. Spruijt and co-workers developed redox-active coacervates via phase separation of cationic peptides (polylysine and polyarginine) and prebiotically relevant ferricyanide ($Fe(CN)_6^{3-}$) molecules (Figure 8b).[79] The oxidizing potential of ($Fe(CN)_6^{3-}$)

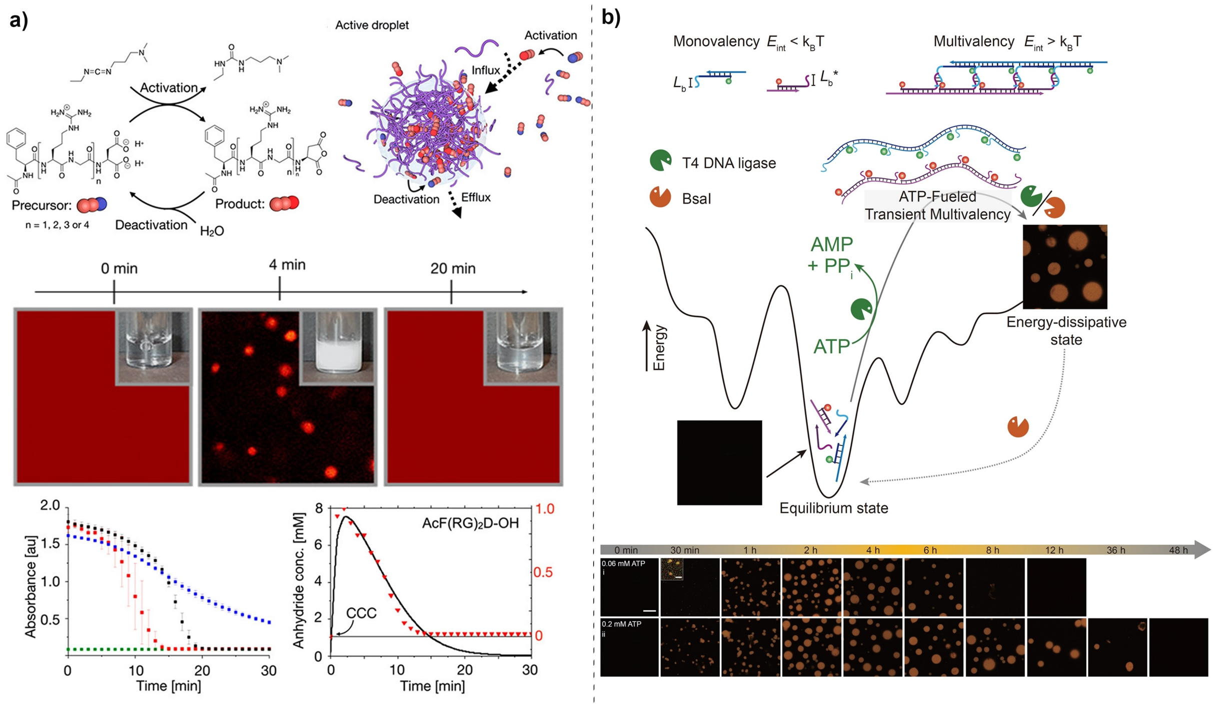

Figure 7. a) Top: Scheme illustration of engineering transient coacervates with charged peptide and polystyrenesulfonate, regulated by EDC addition and product hydrolysis after prolonged incubation. Middle: Confocal laser scanning microscopy micrographs showed that the addition of EDC fueled the formation of transient coacervate droplets, which disassembled upon prolonged incubation (Red colored is sulforhodamine). Down: Absorption intensity of solutions (with $n=1,2,3,4$ in peptides) decreased while the amount of anhydride (with $n=2$ in peptide) underwent an initial increase and subsequent decrease upon the addition of EDC and followed hydrolysis. Reproduced from Ref. [76] with permission, Copyright 2021, American Chemical Society. b) Formation of transient all-DNA coacervates with ATP as a fuel to drive the LLPS and coacervates disappeared upon the consumption of ATP in a fuel-driven process. Reproduced from Ref. [77] with permission, Copyright 2020, Elsevier.

inside coacervates is beneficial for new amide bond formation between prebiotically relevant amino acids and α-amidothioacids. This led further to the formation of fibrous networks within the coacervates in a spatially controlled manner. Future work about engineering synthetic coacervates as catalytic compartments should focus on enhancing their catalyst loading efficiency and spatial organization to optimize reaction rates and selectivity. Tandem reactions or cascade catalytic pathways within coacervates should be further explored to enable complex biochemical reactions, similar to natural metabolic pathways.

5.2. Biomedical Delivery in Vitro and in Vivo

Synthetic coacervates demonstrate a robust ability to sequestrate and concentrate a variety of functional species, including molecular catalysts and drugs, macromolecular proteins and RNAs, and active nanoparticles of distinct molecular sizes and properties.[10b,19a] Compared to conventional inorganic and polymeric nanoplatforms with limited encapsulation capacities, synthetic coacervates are emerging as more versatile encapsulation and delivery systems.[9a,80] Additionally, the dynamic assembly and disassembly behaviors of synthetic coacervates, facilitated by the integration of responsive modules, enable fine regulation of the release of internal cargoes in response to various stimuli and specific physiological conditions (such as light, enzymes, pH value, and redox levels).[13b,73,80a] These unique features allow synthetic coacervates to not only construct biomimetic systems for studying complex biochemical pathways but also develop emergent biotechnological applications. The design of dynamic coacervates with physiological condition responsiveness enables precisely controlled cargo release in the disease region.[80a] This is crucial for boosting therapeutic efficiency while reducing off-target effects. By designing coacervate-forming components with specific functional groups, their behavior can be programmed for specific tasks, such as diagnostic sensing or therapeutic delivery in biomedical fields.[81]

Synthetic coacervates have been designed to sense the physical stimuli, intracellular microenvironment, or biological cues and act accordingly. Xia and co-workers designed a photo-responsive phase-separating fluorescent molecule that displayed LLPS as fluorescent droplets in the aqueous solution, which displayed recruitment towards a wide range of peptides and proteins (Figure 9a).[82] Upon intracellular transport of proteins via transmembrane delivery and irradiation with a 405 nm laser, the fluorescent droplets disintegrate which dispersed the payloads from condensates into the cytosolic space. Synthetic coacervates can also be designed with responsiveness to physiological stimuli, which renders them ideally compatible with biomedical-related applications. Miserez and co-workers dem-

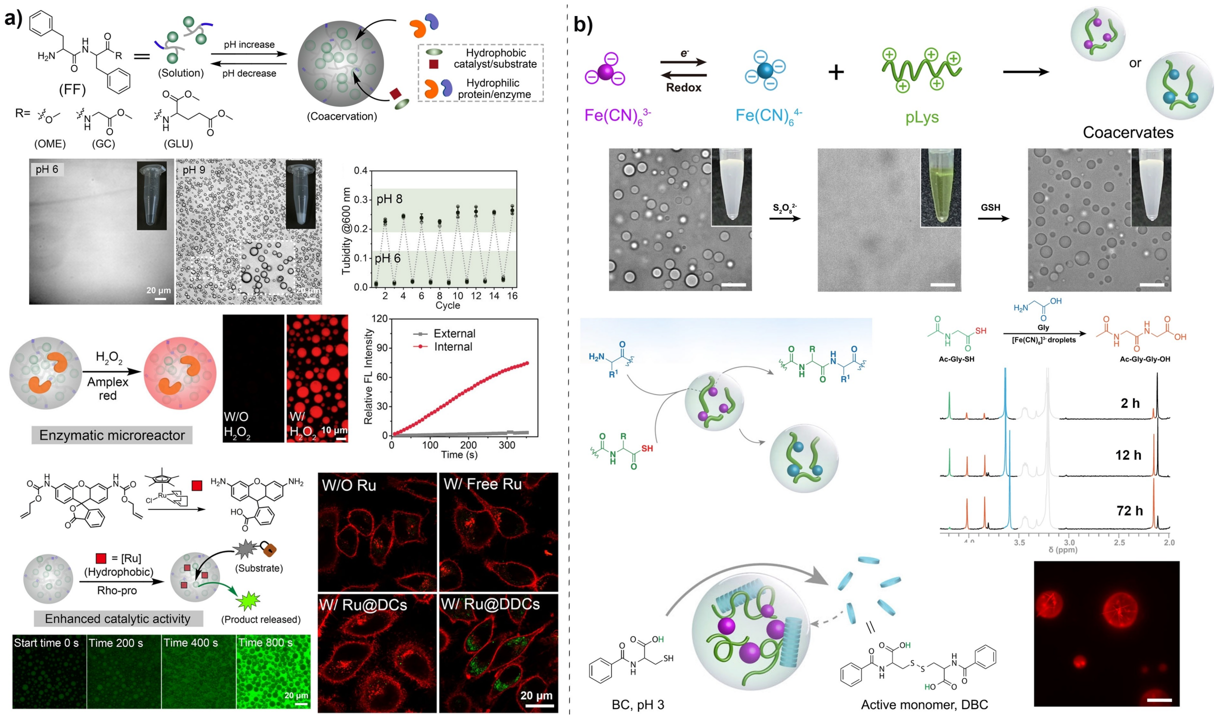

Figure 8. a) Top: Scheme illustration of the formation of short-peptide-based liquid droplets, the peptide coacervates are reversible dependent on environmental pH values; Middle: The peptide coacervates were utilized as a micro-reactor catalyzing Amplex-red into resorufin, which mainly distributed inside the coacervates; Down: The peptide coacervates were capable to catalyze bio-orthogonal reaction via encapsulating a Ruthenium catalyst, which produced emissive product and release into the surroundings. The bio-orthogonal reaction can be translocated into living cells. Reproduced from Ref. [50b] with permission, Copyright 2024, Springer Nature. b) Top: Complex coacervates between $Fe(CN)_6^{4-}$ and polylysine displayed oxidation-reduction responsiveness. Middle: The complex coacervates can be utilized as a reaction center for peptide synthesis. Down: The oxidation of peptides led to solid fiber formation inside liquid coacervates. Reproduced from Ref. [79] with permission, Copyright 2024, Springer Nature.

onstrated such an example of pH-induced coacervation of a histidine-rich polypeptide HBpep that is conjugated with a disulfide-bond linkage (Figure 9b).[80a] The polypeptide coacervates displayed partitioning and concentration towards a wide range of biomacromolecules including small peptides (~720 Da), enzymes as large as 430 kDa, and mRNAs (mRNAs). Upon internalization into the cells, the peptide coacervates due to their liquid property were able to directly cross the cellular membrane and enter the cytosol, bypassing classical endocytic pathways. Macromolecular cargoes or therapeutic agents (e.g., BSA, β-Gal, EGFP, Saporin, and Lysozyme) were subsequently released via intracellular GSH-induced chain cleavage and coacervates disassemble. The biological activities of cellular internalized cargoes are maintained, as the delivered mRNA displayed a high transfection efficiency. The coacervate-based delivery system that can allow direct delivery of active biomacromolecules and avoid endosome trap represent a promising delivery platform in biomedical fields.

Coacervate droplets upon membranization displayed enhanced stability and increased biocompatibility, while also enabling gated membrane transportation and surface functionalization. This strategy can be utilized to increase the biocompatibility and biological function of membrane-bound coacervate droplets, rendering potential utilities for *in vivo* applications. Mann and co-workers demonstrated erythrocyte membrane fragments modified coacervate droplets, which exhibited high haemocompatibility and improved blood circulation time compared with the membrane-free control (Figure 10).[83] Encapsulation of hemoglobin and glucose oxidase within the coacervates was further exploited for the generation of nitric oxide (NO) flux in vivo for blood vessel vasodilation. The design and construction of coacervate-based delivery systems provide new opportunities and innovative solutions in the biomedical field, such as towards the treatment of various pathologies including metabolic diseases and cancer.

6. Summary and Outlook

Synthetic coacervate droplets, formed via liquid-liquid phase separation procedures demonstrate remarkable similarity to the features and properties of biomolecular condensates. They offer unique advantages including a dynamic nature, the ability to mimic cellular compartmentalization, and tunable properties. These unique properties make synthetic coacervates a valuable framework for facilitating the study of molecular interactions and fundamental principles underlying the formation of biological condensates. Via adapting biological principles and replicating the cellular structure and organization features, synthetic coacervates serve as

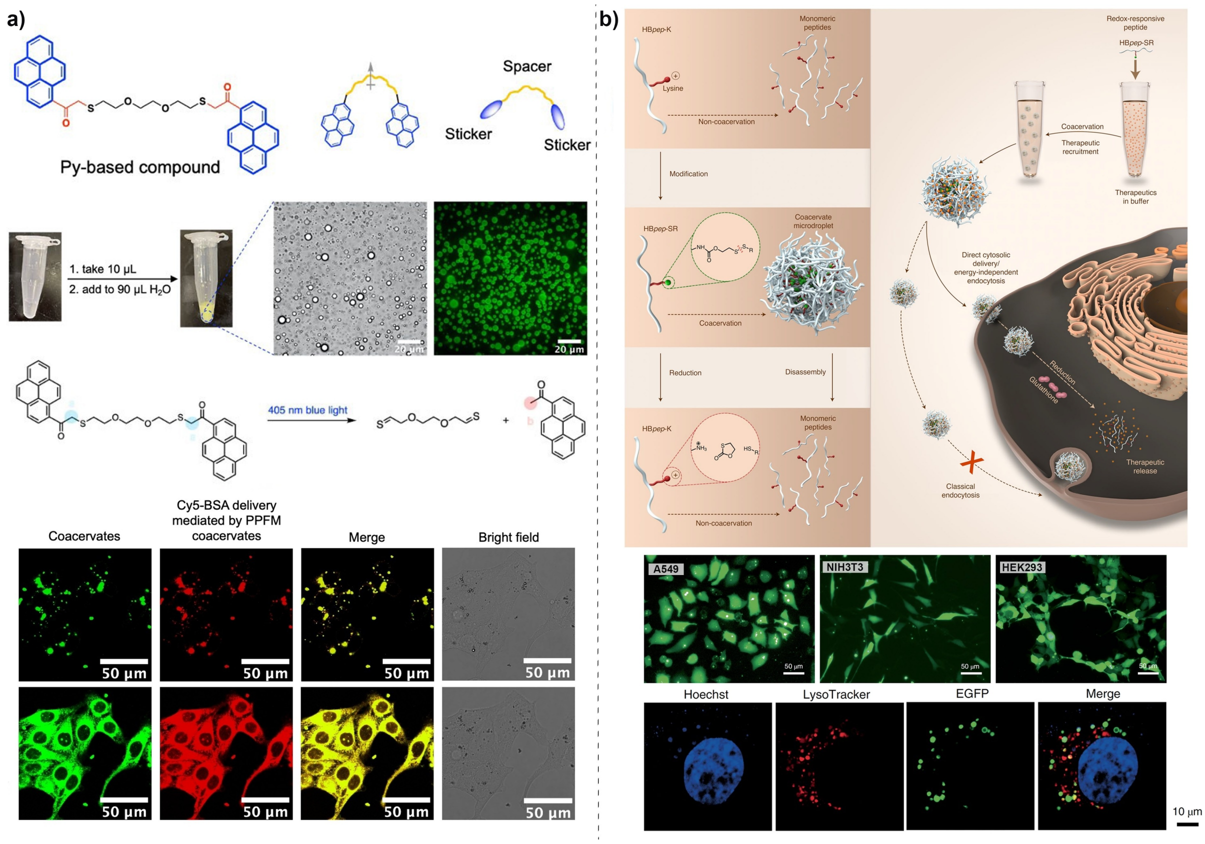

Figure 9. a) Top: Fluorescent molecules based on pyrene adapting a sticker-spacer structure showed phase-separating behaviors into coacervate droplets (green color indicated the pyrene emission). Middle: the fluorescent molecules showed photo-responsiveness which underwent bond cleavage upon UV light irradiation. Down: Upon cellular internalization and light-irradiation, light-responsiveness enabled controlled release of encapsulated protein from the coacervates (green: coacervate; red: Cy5-BSA). Reproduced from Ref. [82] with permission, Copyright 2023. b) Top: Scheme illustration of disulfide-bond integrated histidine-rich polypeptide coacervates, which showed direct transmembrane transportation and GSH-mediated release. Middle: The peptide-coacervates were capable of effectively delivering EGFP into various cell lines. Down: Upon internalization, the coacervates (encapsulating EGFP) were not co-localized with lysosomes. Reproduced from Ref. [80a] with permission, Copyright 2023, Springer Nature.

excellent platforms to recreate and study complex biochemical pathways and interactions within an artificial compartmentalized environment. Advances in this area will enhance our understanding of intracellular processes, such as signal transduction, metabolic pathways, and the formation of membraneless organelles. Developing more sophisticated cytomimetic models will bridge the gap between in vitro studies and in vivo biological complexity.

Compared with conventional delivery vehicles such as polymer-drug conjugates, liposomes, polymersomes and silica nanoparticles, synthetic coacervates due to their unique features present a range of distinct advantages, making them highly attractive for advanced biomedical and biotechnological applications. For instance, coacervate droplets can facilely sequestrate a wide range of functional species including therapeutic drugs, hydrophilic proteins/enzymes, hydrophobic catalysts, RNAs, and active nanoparticles with different polarities and molecular sizes. This makes coacervate droplets a more versatile encapsulation platform that can co-delivery different therapeutic agents, opening up new possibilities for combination therapies. Conventional nanosized delivery systems with solid features are often internalized by cells via endocytosis-based pathways as major uptake mechanisms. The flexibility, softness, and liquid features of synthetic coacervates offered alternative cellular internalization mechanisms and pathways such as the directed transmembrane delivery. In addition, dynamic control of synthetic coacervates offers significant opportunities and innovative solutions for developing biomimicry and biotechnological applications. Through the manipulation of phase-separation mechanisms, stimuli-responsive behavior and design modulation, synthetic coacervate droplets can be facilely tailored and manipulated for specific functions. The ability of coacervate droplets to reversibly self-assemble through phase separation offers high dynamicity and remarkable tunability, allowing for the design of responsive systems that adapt to environmental triggers such as pH, temperature, or biological factors. This feature makes coacervate droplets particularly well-suited for controlled drug delivery, enabling precise therapeutic release in response to specific physiological conditions. Furthermore, their crowded interiors mimic living cells and promote biochemical interactions and reaction rates, making them ideal candidates for constructing artificial organelles or

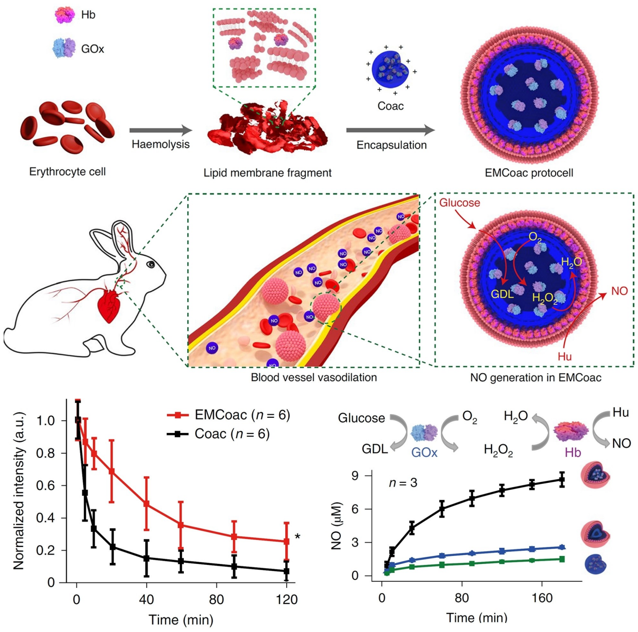

Figure 10. Top: Scheme illustration of erythrocyte membrane-enclosed coacervate protocells which can be used for NO production and blood vessel vasodilation in the rabbit. Down left: The membrane-coated coacervates showed a prolonger circulation profile compared with naked coacervates. Down right: Membrane-enclosed coacervates showed an increase in NO production compared with the controls (without Gox or membrane). Reproduced from Ref. [83] with permission, Copyright 2020, Springer Nature.

compartmentalized systems for efficient biocatalysis and metabolic engineering. The potential of synthetic biomolecular condensates is vast, encompassing catalytic microreactor, cellular delivery, diagnostic sensing, and therapeutic applications. Their versatile synthesis, dynamic nature, compartmentalization ability, and tunable responsiveness to physiological stimuli make them highly suitable for therapeutic delivery, controlled release, and target therapy in biomedical applications.

Considerable challenges remain in further harnessing the potential of synthetic coacervates for biomimetic systems and advanced materials with sophisticated functions. Important parameters such as stability, control over composition, selective permeability, functional integration, scalability, and reproducibility need to be carefully examined. It is of significant importance to investigate the 'structure-dynamics-biological function' relationships of synthetic coacervates to understand their interactions and integration with living systems (including *in vitro* uptake and *in vivo* circulation). Improved stability, optimizing size for *in vivo* applications, and enhancing targeted delivery are critical criteria for their successful development in further biomedical applications. In addition, avoiding premature release and controlled degradation are also important factors that need to be considered in medicine and biotechnology. Addressing these challenges in harnessing synthetic coacervates for advanced biomimetic systems and materials requires a multi-faceted approach. Enhancing stability can be achieved by incorporating cross-linking strategies or by designing more robust coacervate systems that resist environmental fluctuations. Controlling composition and selective permeability may be improved through the precise design of polymer or peptide components, allowing for tunable interactions and selective transport of molecules. Embedding bioactive molecules, enzymes, or responsive elements within the coacervates should be considered to enable complex functions such as controlled drug release, catalysis, or signaling. Standardized and efficient synthesis methods, possibly leveraging microfluidics or high-throughput techniques are required to enhance the scalability and reproducibility. To optimize *in vivo* performance, adjusting the size of coacervates for better circulation and uptake, alongside the use of targeting ligands, will enhance their ability to reach specific tissues or cells. Additionally, designing coacervates with controlled degradation profiles and mechanisms to prevent premature release will further ensure their efficacy in biomedical applications. Ultimately, understanding the structure-dynamics-function relationships through in-depth research and tailoring coacervate properties to specific applications will be crucial for overcoming these challenges. Continued research and development in this emerging field hold the promise of gaining deeper insights into the fundamental principles of life, revolutionizing our approach to biomimicry and therapeutic delivery, and developing innovative technologies that leverage life-like behaviors for practical applications.

Acknowledgements

This work is supported by the National Natural Science Foundation of China (12302410, 52403198), the Sichuan Science and Technology Program (2024YFHZ0356), and the Fundamental Research Funds for the Central Universities. This work is part of the research conducted within the Max Planck Consortium for Synthetic Biology (MaxSynBio) jointly funded by the Federal Ministry of Education and Research of Germany (BMBF) and the Max Planck Society. Open Access funding enabled and organized by Projekt DEAL.

Conflict of Interest

The authors declare no conflict of interest.

Data Availability Statement

The data that support the findings of this study are available from the corresponding author upon reasonable request.

Keywords: Biomolecular condensates · Synthetic coacervates · Cytomimetic modelling · Dynamic control · Biomedical delivery

[1] a) D. Bracha, M. T. Walls, C. P. Brangwynne, *Nat. Biotechnol.* **2019**, *37*, 1435–1445; b) Y. Shin, C. P. Brangwynne, *Science* **2017**, *357*, eaaf4382.
[2] a) C. Roden, A. S. Gladfelter, *Nat. Rev. Mol. Cell Biol.* **2021**, *22*, 183–195; b) Y. F. Gao, X. Li, P. L. Li, Y. Lin, *Nat. Chem. Biol.* **2022**, *18*, 1307–1318.
[3] a) L.-P. Bergeron-Sandoval, N. Safaee, S. W. Michnick, *Cell* **2016**, *165*, 1067–1079; b) B. Monterroso, W. Margolin, A. J. Boersma, G. Rivas, B. Poolman, S. Zorrilla, *Chem. Rev.* **2024**, *124*, 1899–1949.
[4] L. Bar-Peled, N. Kory, *Nat. Metab.* **2022**, *4*, 1232–1244.
[5] a) S. F. Banani, H. O. Lee, A. A. Hyman, M. K. Rosen, *Nat. Rev. Mol. Cell Biol.* **2017**, *18*, 285–298; b) Q. Su, S. Mehta, J. Zhang, *Mol. Cell* **2021**, *81*, 4137–4146.
[6] a) C. P. Brangwynne, C. R. Eckmann, D. S. Courson, A. Rybarska, C. Hoege, J. Gharakhani, F. Jülicher, A. A. Hyman, *Science* **2009**, *324*, 1729–1732; b) J. Söding, D. Zwicker, S. Sohrabi-Jahromi, M. Boehning, J. Kirschbaum, *Trends Cell Biol.* **2020**, *30*, 4–14.
[7] a) M. Carmo-Fonseca, *Cell* **2002**, *108*, 513–521; b) A. S. Lyon, W. B. Peeples, M. K. Rosen, *Nat. Rev. Mol. Cell Biol.* **2021**, *22*, 215–235.
[8] a) S. Mehta, J. Zhang, *Nat. Rev. Cancer.* **2022**, *22*, 239–252; b) J. L. Silva, D. Foguel, V. F. Ferreira, T. C. R. G. Vieira, M. A. Marques, G. D. S. Ferretti, T. F. Outeiro, Y. Cordeiro, G. A. P. de Oliveira, *Chem. Rev.* **2023**, *123*, 9094–9138.
[9] a) Y. Dai, L. You, A. Chilkoti, *Nat. Rev. Bioeng.* **2023**, *1*, 466–480; b) S. Lim, D. S. Clark, *Trends Biotechnol.* **2024**, *42*, 496–509.
[10] a) A. B. Cook, S. Novosedlik, J. C. M. van Hest, *Acc. Mater. Res.* **2023**, *4*, 287–298; b) N. A. Yewdall, A. A. M. André, T. Lu, E. Spruijt, *Curr. Opin. Colloid Interface Sci.* **2021**, *52*, 101416; c) M. Abbas, W. P. Lipiński, J. Wang, E. Spruijt, *Chem. Soc. Rev.* **2021**, *50*, 3690–3705; d) C. Xu, N. Martin, M. Li, S. Mann, *Nature* **2022**, *609*, 1029–1037.
[11] a) A. Abyzov, M. Blackledge, M. Zweckstetter, *Chem. Rev.* **2022**, *122*, 6719–6748; b) A. Samanta, L. Baranda Pellejero, M. Masukawa, A. Walther, *Nat. Chem. Rev.* **2024**, *8*, 454–470; c) W. J. Altenburg, N. A. Yewdall, D. F. M. Vervoort, M. H. M. E. van Stevendaal, A. F. Mason, J. C. M. van Hest, *Nat. Commun.* **2020**, *11*, 6282.
[12] a) A. Jain, S. Kassem, R. S. Fisher, B. Wang, T.-D. Li, T. Wang, Y. He, S. Elbaum-Garfinkle, R. V. Ulijn, *J. Am. Chem. Soc.* **2022**, *144*, 15002–15007; b) S. Deshpande, F. Brandenburg, A. Lau, M. G. F. Last, W. K. Spoelstra, L. Reese, S. Wunnava, M. Dogterom, C. Dekker, *Nat. Commun.* **2019**, *10*, 1800.
[13] a) Y. Yan, W. Mu, H. Li, C. Song, Y. Qiao, Y. Lin, *Adv. Mater.* **2023**, *35*, 2210700; b) H. Karoui, M. J. Seck, N. Martin, *Chem. Sci.* **2021**, *12*, 2794–2802; c) A. B. Cook, B. D. Gonzalez, J. C. M. van Hest, *Biomacromolecules* **2024**, *25*, 425–435.
[14] a) E. Rideau, R. Dimova, P. Schwille, F. R. Wurm, K. Landfester, *Chem. Soc. Rev.* **2018**, *47*, 8572–8610; b) Z. Liu, W. Zhou, C. Qi, T. T. Kong, *Adv. Mater.* **2020**, *32*, 2002932; c) C. Guindani, L. C. da Silva, S. Cao, T. Ivanov, K. Landfester, *Angew. Chem. Int. Ed.* **2022**, *61*, e202110855; d) Y. Altay, S. Cao, H. Che, L. K. E. A. Abdelmohsen, J. C. M. van Hest, *Biomacromolecules* **2019**, *20*, 4053–4064.
[15] H.-X. Zhou, D. Kota, S. Qin, R. Prasad, *Chem. Rev.* **2024**, *124*, 8550–8595.
[16] C. P. Brangwynne, P. Tompa, R. V. Pappu, *Nat. Phys.* **2015**, *11*, 899–904.
[17] a) Y. Dai, C. F. Chamberlayne, M. S. Messina, C. J. Chang, R. N. Zare, L. You, A. Chilkoti, *Chem* **2023**, *9*, 1594–1609; b) S. Song, A. Llopis-Lorente, A. F. Mason, L. K. E. A. Abdelmohsen, J. C. M. van Hest, *J. Am. Chem. Soc.* **2022**, *144*, 13831–13838; c) M. Abbas, J. O. Law, S. N. Grellscheid, W. T. S. Huck, E. Spruijt, *Adv. Mater.* **2022**, *34*, 2202913; d) U. Capasso Palmiero, C. Paganini, M. R. G. Kopp, M. Linsenmeier, A. M. Küffner, P. Arosio, *Adv. Mater.* **2022**, *34*, 2104837.
[18] a) I. B. A. Smokers, B. S. Visser, A. D. Slootbeek, W. T. S. Huck, E. Spruijt, *Acc. Chem. Res.* **2024**, *57*, 1885–1895; b) R. R. Poudyal, R. M. Guth-Metzler, A. J. Veenis, E. A. Frankel, C. D. Keating, P. C. Bevilacqua, *Nat. Commun.* **2019**, *10*, 490; c) J. Liu, L. Tian, Y. Qiao, S. Zhou, A. J. Patil, K. Wang, M. Li, S. Mann, *Angew. Chem. Int. Ed.* **2020**, *59*, 6853–6859.
[19] a) Y. Qiao, M. Li, R. Booth, S. Mann, *Nat. Chem.* **2017**, *9*, 110–119; b) Y. Qiao, M. Li, D. Qiu, S. Mann, *Angew. Chem. Int. Ed.* **2019**, *58*, 17758–17763; c) R. Kubota, S. Torigoe, I. Hamachi, *J. Am. Chem. Soc.* **2022**, *144*, 15155–15164; d) M. Li, B. M. Park, X. Dai, Y. Xu, J. Huang, F. Sun, *Nat. Commun.* **2022**, *13*, 3197; e) N. Gao, C. Xu, Z. Yin, M. Li, S. Mann, *J. Am. Chem. Soc.* **2022**, *144*, 3855–3862.
[20] a) L. R. Ganser, A. G. Niaki, X. Yuan, E. Huang, D. Deng, N. A. Djaja, Y. Ge, A. Craig, O. Langlois, S. Myong, *Structure* **2024**, *32*, 177–187.e175; b) M. Linsenmeier, L. Faltova, C. Morelli, U. Capasso Palmiero, C. Seiffert, A. M. Küffner, D. Pinotsi, J. Zhou, R. Mezzenga, P. Arosio, *Nat. Chem.* **2023**, *15*, 1340–1349; c) P. Li, J. Chen, X. Wang, Z. Su, M. Gao, Y. Huang, *Neurobiol. Dis.* **2023**, *183*, 106167.
[21] a) H. R. Kilgore, R. A. Young, *Nat. Chem. Biol.* **2022**, *18*, 1298–1306; b) J. Wang, J.-M. Choi, A. S. Holehouse, H. O. Lee, X. Zhang, M. Jahnel, S. Maharana, R. Lemaitre, A. Pozniakovsky, D. Drechsel, I. Poser, R. V. Pappu, S. Alberti, A. A. Hyman, *Cell* **2018**, *174*, 688–699.
[22] a) Y. F. Dai, M. Farag, D. Lee, X. Z. Zeng, K. Kim, H. I. Son, X. Guo, J. Su, N. Peterson, J. Mohammed, M. Ney, D. M. Shapiro, R. V. Pappu, A. Chilkoti, L. C. You, *Nat. Chem. Biol.* **2023**, *19*, 518–528; b) K. M. Ruff, Y. H. Choi, D. Cox, A. R. Ormsby, Y. Myung, D. B. Ascher, S. E. Radford, R. V. Pappu, D. M. Hatters, *Mol. Cell* **2022**, *82*, 3193–3208.e3198.
[23] a) S. Jain, J. R. Wheeler, R. W. Walters, A. Agrawal, A. Barsic, R. Parker, *Cell* **2016**, *164*, 487–498; b) B. Wang, H. Zhang, J. Huai, F. Peng, J. Wu, R. Lin, X. Fang, *Nat. Chem. Biol.* **2022**, *18*, 1361–1369.
[24] a) J. M. Burke, O. C. Ratnayake, J. M. Watkins, R. Perera, R. Parker, *Sci. Adv.* **2024**, *10*, eadk8152; b) D. S. W. Protter, R. Parker, *Trends Cell Biol.* **2016**, *26*, 668–679.
[25] F. P. Cakmak, S. Choi, M. O. Meyer, P. C. Bevilacqua, C. D. Keating, *Nat. Commun.* **2020**, *11*, 5949.
[26] a) N. Gao, S. Mann, *Acc. Chem. Res.* **2023**, *56*, 297–307; b) E. Sokolova, E. Spruijt, M. M. K. Hansen, E. Dubuc, J. Groen, V. Chokkalingam, A. Piruska, H. A. Heus, W. T. S. Huck, *Proc. Natl. Acad. Sci. USA* **2013**, *110*, 11692–11697; c) A. F. Mason, J. C. M. van Hest, *Emerg. Top. Life Sci.* **2019**, *3*, 567–571; d) A. Perro, N. Coudon, J.-P. Chapel, N. Martin, L. Béven, J.-P. Douliez, *J. Colloid Interface Sci.* **2022**, *613*, 681–696.
[27] a) S. Rekhi, C. G. Garcia, M. Barai, A. Rizuan, B. S. Schuster, K. L. Kiick, J. Mittal, *Nat. Chem.* **2024**, *16*, 1113–1124; b) G. L. Dignon, R. B. Best, J. Mittal, *Annu. Rev. Phys. Chem.* **2020**, *71*, 53–75; c) A. Boija, I. A. Klein, R. A. Young, *Cancer Cell* **2021**, *39*, 174–192.
[28] a) Z. Lin, T. Beneyton, J. C. Baret, N. Martin, *Small Methods* **2023**, *7*, 2300496; b) Z. F. Wang, M. Zhang, Y. Zhou, Y. W. Zhang, K. M. Wang, J. B. Liu, *Small Methods* **2023**, *7*, e2300042; c) M. Naz, L. Zhang, C. Chen, S. Yang, H. Dou, S. Mann, J. Li, *Commun. Chem.* **2024**, *7*, 79.
[29] Y. Chao, H. C. Shum, *Chem. Soc. Rev.* **2020**, *49*, 114–142.
[30] a) C. Schvartzman, H. Zhao, E. Ibarboure, V. Ibrahimova, E. Garanger, S. Lecommandoux, *Adv. Mater.* **2023**, *35*, 2301856; b) Y. Zhang, Z. Wang, M. Li, C. Xu, N. Gao, Z. Yin, K. Wang, S. Mann, J. Liu, *J. Am. Chem. Soc.* **2023**, *145*, 10396–10403; c) C. Donau, F. Späth, M. Sosson, B. A. K. Kriebisch, F. Schnitter, M. Tena-Solsona, H.-S. Kang, E. Salibi, M. Sattler,

H. Mutschler, J. Boekhoven, *Nat. Commun.* **2020**, *11*, 5167; d) Y. Shen, F. S. Ruggeri, D. Vigolo, A. Kamada, S. Qamar, A. Levin, C. Iserman, S. Alberti, P. S. George-Hyslop, T. P. J. Knowles, *Nat. Nanotechnol.* **2020**, *15*, 841–847.

[31] K. Deepankumar, Q. Guo, H. Mohanram, J. Lim, Y. Mu, K. Pervushin, J. Yu, A. Miserez, *Adv. Mater.* **2022**, *34*, 2103828.

[32] a) S. Koga, D. S. Williams, A. W. Perriman, S. Mann, *Nat. Chem.* **2011**, *3*, 720–724; b) W. A. Scott, E. G. Gharakhanian, A. G. Bell, D. Evans, E. Barun, K. N. Houk, T. J. Deming, *J. Am. Chem. Soc.* **2021**, *143*, 18196–18203; c) T. Lu, E. Spruijt, *J. Am. Chem. Soc.* **2020**, *142*, 2905–2914.

[33] M. Abbas, W. P. Lipinski, K. K. Nakashima, W. T. S. Huck, E. Spruijt, *Nat. Chem.* **2021**, *13*, 1046–1054.

[34] T. Lu, S. Javed, C. Bonfio, E. Spruijt, *Small Methods* **2023**, *7*, 2300294.

[35] a) B. C. Buddingh', J. C. M. van Hest, *Acc. Chem. Res.* **2017**, *50*, 769–777; b) R. Saha, J. A. Choi, I. A. Chen, *Acc. Chem. Res.* **2024**, *57*, 2058–2066.

[36] N.-N. Deng, M. A. Vibhute, L. Zheng, H. Zhao, M. Yelleswarapu, W. T. S. Huck, *J. Am. Chem. Soc.* **2018**, *140*, 7399–7402.

[37] a) W. Mu, L. Jia, M. Zhou, J. Wu, Y. Lin, S. Mann, Y. Qiao, *Nat. Chem.* **2024**, *16*, 158–167; b) T. Ukmar-Godec, S. Hutten, M. P. Grieshop, N. Rezaei-Ghaleh, M.-S. Cima-Omori, J. Biernat, E. Mandelkow, J. Söding, D. Dormann, M. Zweckstetter, *Nat. Commun.* **2019**, *10*, 2909.

[38] a) B. Drobot, J. M. Iglesias-Artola, K. Le Vay, V. Mayr, M. Kar, M. Kreysing, H. Mutschler, T. Y. D. Tang, *Nat. Commun.* **2018**, *9*, 3643; b) T. Y. Dora Tang, D. van Swaay, A. deMello, J. L. Ross Anderson, S. Mann, *Chem. Commun.* **2015**, *51*, 11429–11432.

[39] F. M. Kelley, B. Favetta, R. M. Regy, J. Mittal, B. S. Schuster, *Proc. Natl. Acad. Sci. USA* **2021**, *118*, e2109967118.

[40] a) N.-N. Deng, W. T. S. Huck, *Angew. Chem. Int. Ed.* **2017**, *56*, 9736–9740; b) H. Seo, H. Lee, *Nat. Commun.* **2022**, *13*, 5179; c) R. Booth, Y. Qiao, M. Li, S. Mann, *Angew. Chem. Int. Ed.* **2019**, *58*, 9120–9124.

[41] S. Deshpande, C. Dekker, *Curr. Opin. Colloid Interface Sci.* **2021**, *52*, 101419.

[42] W. Mu, Z. Ji, M. Zhou, J. Wu, Y. Lin, Y. Qiao, *Sci. Adv.* **2021**, *7*, eabf9000.

[43] S. Cao, L. C. da Silva, K. Landfester, *Angew. Chem. Int. Ed.* **2022**, *61*, e202205266.

[44] T. Ivanov, S. Cao, N. Bohra, M. de Souza Melchiors, L. Caire da Silva, K. Landfester, *ACS Appl. Mater. Interfaces* **2023**, *15*, 50755–50764.

[45] Q.-H. Zhao, F.-H. Cao, Z.-H. Luo, W. T. S. Huck, N.-N. Deng, *Angew. Chem. Int. Ed.* **2022**, *61*, e202117500.

[46] a) N. A. Yewdall, A. F. Mason, J. C. M. van Hest, *Interface Focus* **2018**, *8*, 20180023; b) C. Alfano, Y. Fichou, K. Huber, M. Weiss, E. Spruijt, S. Ebbinghaus, G. De Luca, M. A. Morando, V. Vetri, P. A. Temussi, A. Pastore, *Chem. Rev.* **2024**, *124*, 3186–3219.

[47] a) Y. Zhang, Y. Chen, X. Yang, X. He, M. Li, S. Liu, K. Wang, J. Liu, S. Mann, *J. Am. Chem. Soc.* **2021**, *143*, 2866–2874; b) A. F. Mason, B. C. Buddingh', D. S. Williams, J. C. M. van Hest, *J. Am. Chem. Soc.* **2017**, *139*, 17309–17312.

[48] M. van Stevendaal, L. Vasiukas, N. A. Yewdall, A. F. Mason, J. C. M. van Hest, *ACS Appl. Mater. Interfaces* **2021**, *13*, 7879–7889.

[49] a) Y. W. Zhang, Y. F. Chen, X. H. Yang, X. X. He, M. Li, S. Y. Liu, K. M. Wang, J. B. Liu, S. Mann, *J. Am. Chem. Soc.* **2021**, *143*, 2866–2874; b) W. M. Aumiller Jr., F. Pir Cakmak, B. W. Davis, C. D. Keating, *Langmuir* **2016**, *32*, 10042–10053; c) F. Pir Cakmak, A. T. Grigas, C. D. Keating, *Langmuir* **2019**, *35*, 7830–7840.

[50] a) A. Jobdeedamrong, S. Cao, I. Harley, D. Crespy, K. Landfester, L. Caire da Silva, *Nanoscale* **2023**, *15*, 2561–2566; b) S. Cao, T. Ivanov, J. Heuer, C. T. J. Ferguson, K. Landfester, L. Caire da Silva, *Nat. Commun.* **2024**, *15*, 39; c) C. Y. Zhao, J. B. Li, S. L. Wang, Z. J. Xu, X. L. Wang, X. M. Liu, L. Wang, X. Huang, *ACS Nano* **2021**, *15*, 10048–10057.

[51] D. L. J. Lafontaine, J. A. Riback, R. Bascetin, C. P. Brangwynne, *Nat. Rev. Mol. Cell Biol.* **2021**, *22*, 165–182.

[52] G. A. Mountain, C. D. Keating, *Biomacromolecules* **2020**, *21*, 630–640.

[53] a) Q. Guo, G. Zou, X. Qian, S. Chen, H. Gao, J. Yu, *Nat. Commun.* **2022**, *13*, 5771; b) X. Liu, A. H. Mokarizadeh, A. Narayanan, P. Mane, A. Pandit, Y.-M. Tseng, M. Tsige, A. Joy, *J. Am. Chem. Soc.* **2023**, *145*, 23109–23120.

[54] S. Choi, M. O. Meyer, P. C. Bevilacqua, C. D. Keating, *Nat. Chem.* **2022**, *14*, 1110–1117.

[55] H. Wu, Y. Qiao, *Supramolecular Materials* **2022**, *1*, 100019.

[56] V. Mukwaya, S. Mann, H. Dou, *Commun. Chem.* **2021**, *4*, 161.

[57] H. Tan, S. Guo, N.-D. Dinh, R. Luo, L. Jin, C.-H. Chen, *Nat. Commun.* **2017**, *8*, 663.

[58] R. S. Fisher, S. Elbaum-Garfinkle, *Nat. Commun.* **2020**, *11*, 4628.

[59] a) A. D. Slootbeek, M. H. I. van Haren, I. B. A. Smokers, E. Spruijt, *Chem. Commun.* **2022**, *58*, 11183–11200; b) M.-Y. Chang, H. Ariyama, W. T. S. Huck, N.-N. Deng, *Chem. Soc. Rev.* **2023**, *52*, 3307–3325; c) M. D. Hardy, J. Yang, J. Selimkhanov, C. M. Cole, L. S. Tsimring, N. K. Devaraj, *Proc. Natl. Acad. Sci. USA* **2015**, *112*, 8187–8192.

[60] A. Samanta, V. Sabatino, T. R. Ward, A. Walther, *Nat. Nanotechnol.* **2020**, *15*, 914–921.

[61] A. Ianeselli, D. Tetiker, J. Stein, A. Kühnlein, C. B. Mast, D. Braun, T. Y. Dora Tang, *Nat. Chem.* **2022**, *14*, 32–39.

[62] P. Zhan, K. Jahnke, N. Liu, K. Göpfrich, *Nat. Chem.* **2022**, *14*, 958–963.

[63] a) S. M. Bartelt, J. Steinkühler, R. Dimova, S. V. Wegner, *Nano Lett.* **2018**, *18*, 7268–7274; b) B. V. V. S. P. Kumar, A. J. Patil, S. Mann, *Nat. Chem.* **2018**, *10*, 1154–1163.

[64] E. Jambon-Puillet, A. Testa, C. Lorenz, R. W. Style, A. A. Rebane, E. R. Dufresne, *Nat. Commun.* **2024**, *15*, 3919.

[65] S. Song, A. F. Mason, R. A. J. Post, M. De Corato, R. Mestre, N. A. Yewdall, S. Cao, R. W. van der Hofstad, S. Sanchez, L. K. E. A. Abdelmohsen, J. C. M. van Hest, *Nat. Commun.* **2021**, *12*, 6897.

[66] L. Jia, S. Gao, Y. Qiao, *Small Methods* **2024**, 2301724.

[67] C. Love, J. Steinkühler, D. T. Gonzales, N. Yandrapalli, T. Robinson, R. Dimova, T.-Y. D. Tang, *Angew. Chem. Int. Ed.* **2020**, *59*, 5950–5957.

[68] C. Lennicke, H. M. Cochemé, *Mol. Cell* **2021**, *81*, 3691–3707.

[69] J. Wang, M. Abbas, Y. Huang, J. Wang, Y. Li, *Commun. Chem.* **2023**, *6*, 243.

[70] T. P. López-Palacios, J. L. Andersen, *Trends Cell Biol.* **2023**, *33*, 649–666.

[71] W. M. Aumiller, C. D. Keating, *Nat. Chem.* **2016**, *8*, 129–137.

[72] K. K. Nakashima, M. H. I. van Haren, A. A. M. André, I. Robu, E. Spruijt, *Nat. Commun.* **2021**, *12*, 3819.

[73] N. Martin, L. Tian, D. Spencer, A. Coutable-Pennarun, J. L. R. Anderson, S. Mann, *Angew. Chem. Int. Ed.* **2019**, *58*, 14594–14598.

[74] a) W.-J. Wang, C.-P. Tan, Z.-W. Mao, *Curr. Opin. Chem. Biol.* **2023**, *74*, 102308; b) W. Sun, J. Yin, L. Liu, Z. Wu, Y. Wang, T. Liu, H. Xiong, X. Liu, X. Wang, H. Jiang, *Anal. Chem.* **2023**, *95*, 14101–14110.

[75] a) Y. Sato, T. Sakamoto, M. Takinoue, *Sci. Adv.* **2020**, *6*, eaba3471; b) T. Lu, K. K. Nakashima, E. Spruijt, *J. Phys. Chem. B* **2021**, *125*, 3080–3091.

[76] F. Späth, C. Donau, A. M. Bergmann, M. Kränzlein, C. V. Synatschke, B. Rieger, J. Boekhoven, *J. Am. Chem. Soc.* **2021**, *143*, 4782–4789.
[77] J. Deng, A. Walther, *Chem* **2020**, *6*, 3329–3343.
[78] a) T. Hirose, K. Ninomiya, S. Nakagawa, T. Yamazaki, *Nat. Rev. Mol. Cell Biol.* **2023**, *24*, 288–304; b) B. R. Sabari, A. Dall'Agnese, R. A. Young, *Trends Biochem. Sci.* **2020**, *45*, 961–977.
[79] J. Wang, M. Abbas, J. Wang, E. Spruijt, *Nat. Commun.* **2023**, *14*, 8492.
[80] a) Y. Sun, S. Y. Lau, Z. W. Lim, S. C. Chang, F. Ghadessy, A. Partridge, A. Miserez, *Nat. Chem.* **2022**, *14*, 274–283; b) S. Cao, L. K. E. A. Abdelmohsen, J. Shao, J. van den Dikkenberg, E. Mastrobattista, D. S. Williams, J. C. M. van Hest, *ACS Macro Lett.* **2018**, *7*, 1394–1399; c) Y. Hou, S. Cao, X. Li, B. Wang, Y. Pei, L. Wang, Z. Pei, *ACS Appl. Mater. Interfaces* **2014**, *6*, 16909–16917; d) S. Cao, J. Shao, Y. Xia, H. Che, Z. Zhong, F. Meng, J. C. M. van Hest, L. K. E. A. Abdelmohsen, D. S. Williams, *Small* **2019**, *15*, 1901849.
[81] a) Y. Sun, X. Xu, L. Chen, W. L. Chew, Y. Ping, A. Miserez, *ACS Nano* **2023**, *17*, 16597–16606; b) S. Yang, H. Yu, X. Xu, T. Yang, Y. Wei, R. Zan, X. Zhang, Q. Ma, H. C. Shum, Y. Song, *ACS Nano* **2023**, *17*, 8195–8203.
[82] Y. Bao, H. Chen, Z. Xu, J. Gao, L. Jiang, J. Xia, *Angew. Chem. Int. Ed.* **2023**, *62*, e202307045.
[83] S. Y. Liu, Y. W. Zhang, M. Li, L. Xiong, Z. J. Zhang, X. H. Yang, X. X. He, K. M. Wang, J. B. Liu, S. Mann, *Nat. Chem.* **2020**, *12*, 1165–1173.

Manuscript received: September 24, 2024
Accepted manuscript online: November 22, 2024
Version of record online: January 23, 2025